

# **INVESTIGATIONS ON OPERATION AND CONTROL OF SELF-EXCITED INDUCTION GENERATOR**

Submitted in partial fulfillment of the requirements for the award of the degree of  
**Doctor of Philosophy**

by

**Duli Chand Meena**  
**Roll No. 2K11/PhD/EE/14**

Under the Supervision of

**Prof. Madhusudan Singh**  
**Department of Electrical Engineering**  
**Delhi Technological University**



**DEPARTMENT OF ELECTRICAL ENGINEERING**  
**DELHI TECHNOLOGICAL UNIVERSITY**  
**DELHI, INDIA**

**MAY, 2022**

© Delhi Technological University-2022  
All Right Reserved

## **CERTIFICATE**

This is to certify that the thesis entitled “**Investigations on Operation and Control of Self-Excited Induction Generator**” being submitted by Duli Chand Meena (2K11/ PhD/EE/14) to the Delhi Technological University, Delhi for the award of the Degree of Doctor of Philosophy is the record of the bonafide research work carried by him under my guidance and supervision. He has fulfilled the requirements which to our knowledge have reached the requisite standard for the submission of this thesis. It is further certified that the work embodied in this thesis has neither partially nor fully submitted to any other University or Institution for the award of any degree or diploma.

Date: 06-05-2022

**Prof. Madhusudan Singh**

Department of Electrical Engineering

Delhi Technological University

New Delhi-110042

## ACKNOWLEDGEMENT

---

With immense pleasure and satisfaction, I would like to thank almighty for giving me thought, clarity, strength, mental stability to start the PhD programme and for blessings to help me raise my academic level to this stage. I pray for their benediction in my future accomplishments.

From the bottom of my heart, I express my sincere thanks and profound gratitude to my research supervisor, Professor (Dr.) Madhusudan Singh, Delhi Technological University and Professor, Department of Electrical Engineering for allowing me to take the research project under his guidance. Working with him has opened a new horizon of state-of-the-art in the area of power quality issues in wind based distributed generation system. Deep insight of Professor Madhusudan Singh about the subject, ample research ideas, vast imagination in electrical engineering, and adaptable exposure in international forum has enormously helped me in carrying out my research. I extend my deep sense of gratitude for his insistent support, stimulus, encouragement and supervision.

I am also thankful to Dr. Ashutosh K Giri, Assistant Professor, Government Engineering College, Bharuch, Gujarat for his time-to-time immense technical support. The valuable inputs provided by him made me more confident and helpful in technical writing.

My earnest thanks to Dr. (Prof.) Uma Nangia, Head, Department of Electrical Engineering, DTU, for her continuous support and for providing infrastructural facilities at the department.

I would also like to thank all my faculty colleagues from EED, DTU for their support, encouragements and help throughout my research work. I would like to share the credit earned during my PhD course among my research colleagues Mr. Sombir Kundu, and Dr. Suryakant Shukla for their valuable assistances and co-operation. More personally, I would like to extend

my thanks to Mr. Upender Kumar, Mr. Ajender Singh for providing and arranging all necessary help in Project and Research laboratory for carrying out experimental work.

I would like to mention my special thanks to DTU administration office, DTU for giving me an opportunity to study the PhD programme. Moreover, I would like to acknowledge my sincere gratitude to Prof. Yogesh Singh, former Vice-chancellor, DTU and Prof. J.P. Saini, Vice-chancellor, DTU for their time-to-time support and motivation to pursue my research work at DTU.

Finally, I would never forget the deepest concern of my parents, my wife Shakuntla, my daughters Pragati, Priyanshi and my son Prateek for their forever love, care and beliefs during the overall journey of research work.

Date: 06-05-2022

Place: Delhi

(Duli Chand Meena)

## ABSTRACT

---

Growing concerns of carbon dioxide emission and environmental pollution motivated the mankind worldwide towards the utilization of green and clean energy. The various energy sources in the green energy domain are wind, solar, biomass, tidal, ocean waves etc. There is a lot of potential to tap the green energy utilizing for medium and low power applications at isolated places of the globe. Due to vast availability of medium and small generators such as self-excited induction generator, brushless DC generator, permanent magnet generators and switched reluctance generator etc., the possibility of power generation from said energy sources enhanced manifold. The basic problem associated with these energy sources are their intermittent power supply nature. However, the matured power electronics technology has provided the viable solution if its proper interface is provided with the main energy source and load. The self-excited induction generator (SEIG) is the natural choice over other generators for three phase medium power applications due to its better electrical and mechanical characteristics. However, the problem of voltage and frequency variation is the concern for researchers at variable loading even at constant power supply from the prime mover turbine. Moreover, due to extensive use of nonlinear circuits in load, power quality problems such as unacceptable level of harmonics in the supply current, load unbalance at the generator terminal, are an additional issue to address. Further, the power electronics devices like active power filters (VSC/ DSTATCOM) are useful to mitigate the aforementioned problems. The operation of these devices is greatly dependent on the feedback controllers working in the current and voltage loops. There are many pulse width modulation techniques available for generating the gate pulses. The controllers in loops are equipped with control algorithms which are getting various feedback electrical signals at its Analog to digital converter (ADC). The selection of

these control algorithms is dependent on their accuracy, speed and capability to extract fundamental components under dynamic loading conditions.

Therefore, this thesis deals with the implementation of a few adaptive control algorithms based on least mean square principle, for improving the performance of Self Excited Induction Generator. The SEIG under study is working in standalone mode to feed power at isolated places and connected to linear/nonlinear load. The major problems associated with such kind of standalone power system is regulation of its voltage and frequency under variable loads. Further, maintaining a purely sinusoidal supply current with improved power factor is also one of the major objectives towards power quality standards. A static compensator (STATCOM) is used along with load to compensate currents to maintain power quality of standalone generator under various operating conditions.

The Leaky-Momentum Control Algorithm (LMA) is being used to generate switching signals. A voltage source converter (VSC) to enhance the performance of a three-phase self-excited induction generator operating with varying loads is used. This LMA technique controls VSC to regulate voltage and frequency of SEIG within a permissible limit. The LMA control is implemented to reduce the higher demand of reactive power, eliminations of harmonics in source current and balancing of loads under different operating conditions. During the electrical and mechanical dynamical conditions, the LMA technique is maintaining a constant voltage and frequency at point of common interfacing (PCI). The proposed technique is a modified control technique of basic Leaky and Momentum Algorithms. This control has removed the drawbacks of Leaky and momentum algorithms. Moreover, it is observed that LMA performs better when there are uncertainties in input conditions.

In the second case, a modified NLMS based control algorithm is designed to control the SEIG system feeding three-phase nonlinear loads. The control algorithm extracts the fundamental weight components with reduced oscillations from sensed load current.

Implementation of modified algorithm for control of voltage source converter (VSC) provides fast dynamic response, harmonic eliminations, active/reactive power compensation, load leveling, rapid convergence and enhances the power quality in an isolated distributed wind energy generation system under nonlinear load conditions. The battery energy storage (BES) is employed at DC Link of STATCOM to balance the power in the system during load perturbations and wind speed changes. The simulation study on the proposed system shows the improved steady state and dynamic performance of SEIG system under fixed/varying wind speed while feeding fixed/varying nonlinear load.

The entire system comprising SEIG, nonlinear load, voltage source converter and battery storage system is implemented in MATLAB /SIMULINK. Also, the experimental validation of proposed control approach is carried out in the laboratory environment to study the effectiveness. It has shown promising performance under both dynamical state and steady state of the system.



# Table of Contents

<b>Certificate</b>	i
<b>Acknowledgment</b>	ii
<b>Abstract</b>	iv
<b>List of Contents</b>	vii
<b>List of Figures</b>	xi
<b>List of Tables</b>	xiii
<b>List of Acronyms</b>	xiv
<b>List of Symbols</b>	xvi
<b>Chapter 1 Introduction and Literature Review</b>	<b>1</b>
1.1 General	1
1.2 Why SEIG is Selected?	1
1.3 The Need of Power Electronics Interface	2
1.4 The Application of Control Algorithms	3
1.5 The Role of Voltage Source Converter	3
1.6 Literature Review: The State of Art	4
1.7 Advantages and Novelities of Proposed Control	10
1.8 Organization of Thesis	11
<b>Chapter 2 Research Objectives and Methodology</b>	<b>12</b>
2.1 General	12
2.2 Research Objectives of the Thesis	12
2.3 Major Contributions	12
2.4 Research Methodology	13
2.4.1 Planning of SEIG based Standalone Generation System	13

2.4.2	Design of Control Algorithms	13
2.4.3	To perform the MATLAB Simulations	14
2.4.4	To perform the Experimentation	14
2.5	Conclusions	14
<b>Chapter 3</b>	<b>SEIG Configuration for Distributed Generation and Estimation of Excitation Capacitance</b>	<b>16</b>
3.1	General	16
3.2	SEIG System Configuration	17
3.3	Method for determining Excitation Capacitance for rated voltage operation of SEIG under Varying Loads	17
3.3.1	Steady State Analysis of SEIG	19
3.3.2	Performance Analysis using Multivariate Newton-Raphson Method	21
3.4	Results and Discussions	23
3.5	Conclusions	26
<b>Chapter 4</b>	<b>Implementation of Leaky-Momentum Control Algorithm for Voltage and Frequency Control of 3-Phase SEIG</b>	<b>27</b>
4.1	General	27
4.2	Leaky Momentum Control Algorithm: An Introduction	28
4.2.1	Weight calculation using LMA Control Algorithm	30
4.2.2	Reference Source current calculation and Gate pulses generation	32
4.3	Simulation Results of SEIG Based Distribution Generation using Leaky Momentum Control Algorithm	32

4.3.1	Generation of Control Signals of VSC using LMA Control Algorithm	33
4.3.2	LMA Control Algorithm Performance for Voltage and Frequency Control under Load Variation on SEIG System	35
4.3.3	Power Balance during sudden change in Load	36
4.3.4	Power Quality Indices in Steady State Conditions	37
4.4	Experimental Performance	39
4.4.1	The Experimental Results under sudden change in System Dynamics	40
4.4.2	The Experimental Performance under Steady State Condition of the system	43
4.5	Conclusions	43
<b>Chapter 5</b>	<b>Implementation of Modified NLMS Control Algorithm for Coordinated Operation in Three-Phase Wind-Energy Conversion System</b>	<b>44</b>
5.1	General	44
5.2	Modified NLMS algorithm: An Introduction	44
5.2.1	Evaluation of Peak value of SEIG terminal voltage, in-phase and quadrature unit vectors	46
5.2.2	Generation of reference source current for VSC	47
5.3	Simulation Study of Modified NLMS Control Algorithm	49
5.3.1	Intermediate Control Signal profiles in NLMS Control Algorithm	51
5.3.2	Steady State Performance of Distributed Generation System Under Fixed Wind Velocity Feeding Fixed Nonlinear Load	52
5.3.3	Dynamic Performance of Distributed Generation System Under Varying Wind Velocity Feeding Fixed Nonlinear Load	52

5.3.4	Dynamic Performance of Distributed Generation System Under Fixed Wind Velocity Feeding Varying Nonlinear Load	53
5.3.5	Power Quality Indices in Steady State Condition/Power Balance Performance in Load Dynamical Conditions	54
5.3.6	Power Quality Analysis of Distributed Generation (DG) System Under Nonlinear Load	56
5.4	Conclusions	58
<b>Chapter 6</b>	<b>Conclusions and Future Scope</b>	<b>60</b>
6.1	Main Conclusions	60
6.2	Future Scope of the Work	61
	<b>APPENDIX A</b>	<b>62</b>
	<b>List of Publications</b>	<b>63</b>
	<b>Author's Biography</b>	<b>64</b>
	<b>References</b>	<b>65</b>

## List of Figures

Fig 3.1	A SEIG coupled to a wind turbine and delivering power to a 3-phase load.	17
Fig. 3.2	Per phase equivalent circuit of SEIG.	20
Fig. 3.3	Variation of load voltage with load current of SEIG at resistive loads.	25
Fig 3.4	Output voltage versus load current under varying inductive loads.	26
Fig. 4.1	Schematic diagram of distributed generation (DG) system based on LMA control algorithm.	27
Fig. 4.2	Block Diagram of LMA control Algorithm	32
Fig. 4.3	Simulation Results of Reference Current Generation Process	33
Fig. 4.4	Simulation Results using LMA Control Algorithm for voltage and Frequency Control of SEIG under Load Variation	36
Fig. 4.5	Simulation performance of LMA during power dynamics of system	37
Fig. 4.6	Simulation Results of Harmonic distortion in steady state (a) THD in phase 'a' of supply voltage (b) THD in phase 'a' of supply current (c) THD in Load current of phase 'a'	38
Fig. 4.7	A photograph of the proto-type experimental set-up developed in laboratory.	40
Fig.4.8	Experimental performance of proposed control with system under study and waveforms of (a) variations in source voltage ( $v_{sa}$ ) with load current dynamics ( $i_{La}$ , $i_{Lb}$ , $i_{Lc}$ ) (b) study of $v_t$ , $f$ , $i_{sa}$ with $i_{La}$ (c) $i_{sa}$ , $i_{La}$ , $i_{Lb}$ , $i_{ca}$ (d) load balancing of $i_{sabc}$ with $i_{La}$ I study of zero sequence current $i_{Tn}$ with load current dynamics ( $i_{La}$ , $i_{Lb}$ , $i_{Lc}$ ), (f) Steady state performance and powers of generator ( $P_g$ ), Load ( $P_L$ ) and battery ( $P_b$ ) and loss in the system.	42
Fig. 5.1	Schematic diagram of distributed generation (DG) system based on Modified NLMS Control Algorithm	47
Fig. 5.2	Block diagram of Modified NLMS control Algorithm	48
Fig. 5.3	Intermediate signals of modified NLMS algorithm (a) active/reactive unit templates, AC terminal voltage PI controller current and DC link voltage PI controller current (b) Extracted active/reactive weight	51

templates, active/reactive reference current (c) active/reactive current component and extracted reference current.

Fig. 5.4	Steady state performance of distributed generation system under fixed wind velocity and fixed load	52
Fig. 5.5	Dynamic performance of distributed generation system under varying wind velocity and fixed load	53
Fig. 5.6	Dynamic performance of distributed generation system under fixed wind velocity and varying load	54
Fig. 5.7	Power quality indices of DG system a) Generated power b) Load power and c) Battery power under fixed/varying wind velocity feeding fixed/varying nonlinear load	556
Fig.5.8	Steady state THD analysis of DG system (a) Source voltage (b) Source current and (c) Load current under nonlinear load condition	58

## **List of Tables**

Table 3.1.	Self-excitation Capacitance requirements under varying resistive loads.	24
Table 3.2	Excitation Capacitance requirements under varying inductive loads (0.8 pf lagging).	25
Table 4.1	Voltage and Frequency Control Operation	36
Table 4.2	Steady State Load Balance Operation	37
Table 4.3	Power Quality Indices in Steady State	39
Table 5.1	Power Balance in different Operating Conditions	56
Table 5.2	Power Quality Indices in Steady State	58

## List of Acronyms

VSC	Voltage source converter
SEIG	Self-excited induction generator
LMS	Least mean squares
PCI	Point of common Interfacing
DSP	Digital signal processor
IGBT	Insulated gate bipolar junction transistor
IRPT	Instantaneous reactive power theory
SRFT	Synchronous reference frame theory
DTC	Direct torque control
ZVR	Zero voltage regulation mode
PFC	Power factor correction
PLL	Phase lock loop
BESS	Battery energy storage system
kW	Kilo watt
kVA	Kilo volt ampere
MW	Mega watt
kVAR	Kilo volt ampere reactive
MVA	Mega volt ampere
DG	Distributed generation
THD	Total harmonic distortion
MLMS	Momentum least mean squares
LMA	Leaky momentum control algorithm
NLMS	New least mean squares
ELC	Electronic load controller
DELIC	Dynamic electronic load controller
STATCOM	Static compensator
DSTATCOM	Distribution static compensator
DVFC	Decoupled voltage and frequency controller
LAF	Lorentzian norm-based adaptive filter
VLLMS	Variable learning and gradient-based least mean squares
LLLAD	Leaky -least logarithmic absolute difference-based algorithm
GIC	Generalized impedance controller



3P4W	Three-phase four wire
GA	Genetic algorithm
NVLF	Non-linear adaptive second-order Volterra filter
KIMEL	Kernel incremental meta-learning control algorithm
SPLL	Software phase lock loop
VCO	Voltage controlled oscillators
VS-PWM	Voltage source- pulse width modulation
LMDT	Leaky minimal disturbance theory-based control
FPGA	Field programmable gate array

## List of Symbols

$v_{sabc}$	Three phase supply voltage in phase ‘a’, ‘b’, ‘c’ respectively in vector notation
$i_{sabc}$	Three phase supply currents in phase ‘a’, ‘b’, ‘c’ respectively in vector notation
$i_{Labc}$	Three phase load currents in phase ‘a’, ‘b’, ‘c’ respectively in vector notation
$i_{Cabc}$	Three phase compensator currents in phase ‘a’, ‘b’, ‘c’ respectively in vector notation
$v_b$	Battery voltage
$i_b$	Battery current
$k$	Noise factor
$\alpha$	Leaky factor
$\varepsilon$	Momentum factor
$\tau_p$	Learning rate
$\sigma$	Error constant factor
$\beta$	Variable regularization factor
$C_{fabc}$	Capacitance of three- phase excitation capacitor bank
$F$	Frequency in Hz
$R$	Load resistance
$L$	Load inductance
$C$	Capacitance
$R_1$	Stator Resistance
$R_2$	Rotor resistance
$X_1$	Stator leakage Reactance
$X_2$	Rotor leakage Reactance
$X_m$	Magnetizing reactance
$X_C$	Excitation capacitive reactance
$C_p$	Power coefficient
$V_W$	Wind velocity
$A$	Swept area of wind turbine
$P_m$	Mechanical power output of the turbine

$\rho$	Air density (kg/m <sup>3</sup> )
$\lambda$	Tip speed ratio
$\omega_R$	Angular velocity in rad/s
$w_{pa}$	Weight of active component of fundamental load current of phase ‘a’
$w_{qa}$	Weight of reactive component of fundamental load current of phase ‘b’
$w_{Lpavg}$	Average magnitude of weighted fundamental active power component
$w_{Lqavg}$	Average magnitude of weighted fundamental reactive power component
$W_p$	Average active weight factor
$W_q$	Average reactive weight factor
$i_{Tn}$	Transformer neutral current
$V_{dc}$	DC link voltage
$W_L$	Leaky weight factor
$W_m$	Momentum weight factor
$P$	Active power
$P_b$	Battery power
$P_L$	Power consumed in load
$P_g$	Generated power
$P_c$	Power from VSC
$V_m$	Peak value of voltage of the wind driven SEIG
$X_c$	Capacitive Reactance
$X_L$	Inductive reactance
$i_{La}, i_{Lb}, i_{Lc}$	Three phase load currents in phase ‘a’, ‘b’, ‘c’ respectively
$i_{sa}, i_{sb}, i_{sc}$	Three phase supply currents in phase ‘a’, ‘b’, ‘c’ respectively
$i_{ca}, i_{cb}, i_{cc}$	Three phase compensator currents in phase ‘a’, ‘b’, ‘c’ respectively
$N_r$	Rotor speed
$Z_L$	Load impedance
$f$	Per unit frequency
$N$	Per unit speed
$u_{pa}$	Single phase voltage unit templates in-phase
$u_{qa}$	Single phase voltage unit templates quadrature-phase
$i_{dp}$	Current component of power loss

$f_s^*$	Reference frequency of source
$f_s$	frequency of source
$f_e(n)$	Frequency error at $n^{\text{th}}$ sampling instant
$n$	Number of samplings
$i_{spt}$	Active power current components amplitude of the reference source current
$\mathbf{i}_{spt}^*$	Active components of the reference source current
$v_t^*$	Reference PCC terminal voltage magnitude at $n^{\text{th}}$ sampling instant
$v_t$	Estimated PCC terminal voltage magnitude at $n^{\text{th}}$ sampling instant
$i_{pd}$	Output of PI controller in frequency control loop
$i_{qq}$	Output of PI controller in voltage control loop
$i_{sqt}$	Amplitude of reactive power current components of the reference source current
$\mathbf{i}_{sqt}^*$	Reactive components of the reference source current
$\mathbf{i}_{sabc}^*$	Three phase estimated reference source current in phase 'a', 'b', 'c' respectively in vector notation
$w_{pa}$	Extracted active weight of load current
$w_{qa}$	Extracted active weight of load current

# CHAPTER 1

## INTRODUCTION AND LITERATURE REVEIW

---

### 1.1 General

The problem of global warming is growing day by day due to exorbitant use of fossil fuels such as coal, oil and natural gas which are major cause of emissions. The emissions of CO<sub>2</sub> due to consumption of fossil fuels to generate electricity is maximum. To reduce greenhouse gas emissions emphasis are now made to produce electricity from renewable energy sources.[1]. The solar, tidal, wind, biomass, etc. can be used for generation of electricity to bring down the effect of global warming [2]. The energy generated from the said non-conventional sources are used for reduction of conventional generation and grid integration [3]. Consequently, it is easy to regulate the frequency and voltage of a complicated power system. Due to recent advancement in the wind technology, the electrical power generation is becoming cost effective, while maintaining system stability and reliability [4]. Conventional power generation in remote and hilly areas is not workable/practicable options of electrical energy generation. Economic growth in the remote isolated areas is set to grow due to development of renewable energy technology [5]. Maintaining grid connected power supply in the remote areas is a costly and difficult proposition. Therefore, the standalone and distributed generations are feasible options to provide electrical supply in remote and hilly areas. Self-excited induction generators (SEIGs), permanent magnet synchronous generators and brushless dc generators have emersed as potential energy conversion machines for increased scope of standalone wind- based energy generation [6].

### 1.2 Why SEIG is Selected?

Due to durability, ruggedness, simple construction, low-maintenance cost in comparison to other machines, SEIG is preferred in wind energy conversion systems for study

purpose [7]. Another good aspect is its capability to retain the residual magnetism after sudden loss of magnetization due to overloading or short circuit. Additionally, it has natural ability to withstand the sudden short circuit without any harm to the stator or rotor windings. The low weight to torque ratio makes it suitable for wind energy system. Also, it has low maintenance cost. The design of the SEIG and its various electrical parameters such as stator and rotor resistances, mutual inductances, self-inductances are least affected when overload or sudden change in load occurs. Therefore, less sensitive and simple controllers which are low-cost work effectively to control the generator voltage and frequency. Hence, SEIG is becoming popular for wind energy conversion system where generators are mounted at higher altitude. But there is issue of poor power quality issues such as frequency variation and change in voltage level with variation in load.

### **1.3 The Need of Power Electronics Interface**

The power electronics technology is playing very important role for making renewable energy system more reliable and controllable. The advancement in the power semiconductor devices technology enhances the possibility to operate the semiconductor switches at higher switching frequency and also at higher power ratings. If the combination of such devices is used as power electronics converters in wind energy system, the reliability and power quality of supply is improved significantly. The switches are also arranged to form various topology of converters such as two level, three level, cascade, hybrid, isolated or multilevel converters depending upon different requirements and applications. There are certain advantages and disadvantages of each converter topology. The need of power electronics interface provides compatibility between various components of the wind energy conversion system. For example, if dc supply is needed for charging the laptop battery, the need of power electronics-based chargers arises. This charger is working as an interfacing device between ac supply and laptop battery. Similarly, there are so many applications need power electronics interface for

improving the energy efficiency and compatibility. But, excessive use of power electronics creates the problem of harmonics injection and poor power quality in the system. However, power electronics can also provide the remedies to power quality issues by some degree. Further, the performance of converter relies on the control techniques/ algorithms used for switching control of converters for its effective working.

#### **1.4 The Application of Control Algorithms**

The controllers in feedback loops of the systems are major component in effective operation and control of any power electronics system. The operation of 3-phase converters used for power quality improvements is governed by classical control techniques based on Park's and Clarke's transformation, Synchronous Reference Frame theory and PQ theory-based techniques, etc. These control algorithms are employed for the generation of reference current and hence generating switching signals to operate the VSC [8]. But these control techniques lack adaptive behavior or their working depends on coefficients of loop gains. Hence control algorithms with adaptiveness are more suitable for wind energy systems.

#### **1.5 The Role of Voltage Source Converter**

The use of SEIG has increased in wind energy generation because of its operation at different speeds. Therefore, electricity can be generated at small scale using low cost small SEIG. The poor voltage and frequency regulation and need for variable reactive power support with varying loads are the two major drawbacks of an induction generator. The use of voltage source converter is needed to support active and reactive power requirements of the SEIG in varying load conditions. There are extensive literatures available to support the above claim. An electronic load compensator (ELC) has been developed to manage constant voltage at a fixed frequency even with variation in consumer loads [9]. Another problem with SEIG is that it draws the non-sinusoidal current from generator terminals and causes distortion of terminal voltage under nonlinear loading conditions. Different current control methods of STATCOM

are being used to control voltage and frequency in a SEIG-based standalone generating system. A dynamic electronic load controller (DELCO) is developed and designed to maintain constant voltage and frequency of a three-phase SEIG [10]. It consists of a VSC which provides variable reactive power under varying load conditions, and hence controls the terminal voltage of SEIG under varying load conditions. The frequency of generator is managed at constant value by dumping excess consumer load in a variable speed AC Drive connected at the DC link of converter. In this scheme two VSC of almost same rating of SEIG is required which is a complex and costly arrangement. Three-phase SEIG in combination with STATCOM is able to feed nonlinear loads up to its rated capacity [11]. By using DSTATCOM as a compensator and sliding mode controller along with proportional and integral controller voltage and power quality issues of a three-phase SEIG under both linear and non-linear loads conditions can be significantly improved [12]. A combination of ELC and STATCOM which is called as Decoupled Voltage and Frequency controller (DVFC) is also used to control the SEIG performances. In DVFC the frequency and voltage of the system is maintained within prescribed range. The DVFC independently controls both frequency and voltage by adjusting real and reactive power at the generator terminal [13]. Applications of DSTATCOM in a distributed power generating system with an SEIG is explained in the literatures. A composite observer-based control algorithm is used for the extraction of fundamental current components in the load [14]. A VSC controlled by implementing Lorentzian norm based adaptive filter (LAF) for power quality enhancement of SEIG in a star-connected three-phase wind based distributed power generating system is also described [15].

## **1.6 Literature Review: The State of Art**

The wind energy system development and its operation with available controllers are provided in literatures. The LAF also neutralizes the effects of wind impulses on the frequency and voltage of generator. The leaky Least mean fourth (LLMF) algorithms are used for the



control of DSTATCOM in solving power quality issues in the grid-connected solar photovoltaic system reported in literature [16]. But the acceleration problem of the convergence process is a major issue. The analysis and basics of momentum least mean squares algorithm (MLMS) is described [17]. The MLMS converges faster because of scaling factor. A Variable Learning and Gradient-based Least Mean Square (VLLMS) algorithm is implemented for control of VSC in a distributed generation [18]. There is no effects of step size, gradient and sensor-noise on convergence performance of VLLMS algorithm due to its insensitivity to these parameters. But in LMS, convergence performance is influenced by step-size parameters.

A novel Leaky-least logarithmic absolute difference (LLLAD)-based control algorithm is experimentally implemented in a PV based system [19]. This technique enhanced the power quality. The MLMS employs additional term called momentum Factor [20]. This factor of the control enhances the converging rate. Also, its tracking competence increases for a signal of non-stationary nature. There are some applications of this control algorithm in distributed power generation system [18-21]. The active and reactive power control technique for SEIG working in standalone mode is described [21]. In nano-grid operations standalone mode supervisory control seems good options [22]. However, due to slow response in randomly changing environment, it is less effective. By using field programmable gate array (FPGA) for peak power point operation, a closed loop control technique has been developed and implemented [23]. A generalized impedance controller (GIC) based speed adaptive stator current compensator control is implemented for the frequency regulation and voltage balance of SEIG in standalone three-phase four wire (3P4W) system [24].

There are few applications which are using simple, robust, accurate and fast dynamics adaptive control techniques but these control applications are either dependent on step size parameters or some independent gain parameters. Therefore, in this thesis attempts have been made to use the combined characteristics of leaky LMS control algorithm and momentum LMS

control algorithm which is more suitable to control the system for random input type of sources such as wind energy system.

Use of evolutionary control algorithm applied in the domain of SEIG research such as a genetic algorithm (GA) technique is also described for steady-state performance analysis instead of using higher order polynomials for the loop or nodal equations [25]. A STATCOM is designed and implemented based on the relative rotation speed theory, which reduces the frequency deviation and maintain synchronism of the system [26]. The STATCOM controls the point of common interface (PCI) voltage through reactive power support and eradicate the harmonics [27]. A simple linear search algorithm and a binary search algorithm are also implemented to operate the SEIG system and control its frequency at a given speed [28]. The non-linear adaptive second-order Volterra filter (NVLF) based adaptive and nonlinear control algorithm is designed to operate voltage source converter (VSC). The NVLF based VSC provides harmonic eradication, power compensation, load leveling and enhance the power quality of the system. The NVLF based control technique has been deployed to evaluate the fundamental load current component for further estimation of reference current [29]. The kernel incremental meta-learning (KIMEL) based control algorithm with DSTATCOM is developed for the extraction of real/reactive weights component and maintains the different parameters of the system [30]. A composite observer-based control algorithm is developed to estimate the fundamental component during distorted current condition and the control algorithm with DSTATCOM maintains the system frequency and voltage at PCI of the generator eliminate harmonics and enhance the power quality of the system [31]. A software phase lock loop (SPLL) control technique is implemented for the extraction of fundamental component of load current and generates the switching pulses for the DSTATCOM [32]. A PLL without VCO has been implemented to generate reference current and this control works both in  $abc$  to  $\alpha\beta$  transforms to reduce the computational burden. The control technique with

VSC provides fast dynamic response and improved power quality under dynamic conditions of wind and nonlinear load [33]. An LCL filter is interfaced between DC-DC converter and battery energy storage (BES) to minimize the ripple current. An additional dump load is used to compensate the disturbances of SEIG under different operating conditions [34]. In reference [35], A DQ based power control algorithm is applied in microgrid system [35]. Genetic algorithm (GA) technique is being used to evaluate the requirements of excitation capacitance to build-up terminal voltage in SEIG at no-load [36]. A perturb & observe MPPT technique is designed to harness maximum power from wind turbine under variation in wind velocity and BES is also used to provide active power support between the source and the load [37]. An adaptive theory based MLMS algorithm is implemented to generate switching pulses for VSC, which provides harmonic eradication, fast response, and enhances the power quality and maintain the system frequency and voltage under varying wind speed/load demand [38]. An MLMS control algorithm is designed to extract fundamental weight component with reduce static error and less oscillations. An MVSS-LMS based adaptive control algorithm is implemented for the accurate estimation of fundamental weight component with speedy convergence and less oscillations [39]. An NLMS based control algorithm is designed to tune the variables regularization factor which accelerates the convergence speed [40]. The concept of droop control mechanism for power balancing among various component of wind energy conversion system is also available [41]. A new power controller is also discussed [42] which is very easy to implement for wind energy system. A VSC with dump load is implemented to maintain the frequency and voltage of SEIG and the dump load is used to consume the extra power under less load demand [43]. The design features of an isolated 3-phase induction generator system are presented and authors have also suggested two stator winding configurations for voltage and frequency regulation from dual stator winding [44]. One more control strategy that consist of static var compensator (SVC) is also presented [45]. The series

compensator concept for improving the transient performance of self-excited induction generator is discussed [46]. Some topology of hybridization of two generators are also proposed [47]. The operation of self-excited induction generator and synchronous generator in parallel is proposed in this article. A comprehensive review on three-phase induction generator is provided [48]. Many SEIG features under in various operating conditions are described in this review. PWM control strategy of VSC is explained and discussed for voltage and frequency regulation of SEIG [49]. The overall efficiency of the generating system is also improved by effective operation of generator. Ojo et al. [50] have suggested the effective utilization of voltage source converter using PWM technique in case of dual stator winding induction generator. This is very effective for separate voltage and frequency control in SEIG. Fukami et al [51] have analyzed the performance of single-phase induction generator using three phase induction machines. It is found to be suitable for different isolated loads where issue of load unbalance is observed. The controlled operation of induction generator in rural applications is presented using VS-PWM technique [52]. The use of bidirectional converter is also suggested for proper power balance. Chen et al. have presented the application of DSTATCOM for voltage and frequency control under random load variations [53]. The control strategy used is very simple and easy to implement. In [54] the evaluation of operating performance for three phase induction generator is presented where practical impedance approach for steady-state analysis in the frequency domain is utilized. Barrado et al. [55] have presented the idea of coordinated operation of STATCOM with bidirectional converter for mitigating the power quality problems of self-excited induction generator. It also provided the flexibility for removing the additional dump load and its controller which was necessary component of conventional controller system for SEIG. Some other configurations such as use of an additional leg in conventional VSC are neutral current compensation under unbalance loading conditions [56]. It has made system very economical and easy to control based on power

balance theory for wind energy applications. In [57], induction generator system is used for voltage and frequency regulation for low and medium power applications. In the Indian power context, a combination of PV generation system and self-excited induction generator is also suggested [58]. This combination is found to be suitable for standalone operation for isolated locations. For obtaining reliable, fast and accurate operation of induction generator, another class of controller named adaptive controllers are presented [59]. These controllers are able to change their gain coefficients or weights for adaptation purpose so that error between actual response and reference quantity can be made zero. The static excitation for dual winding induction generator is presented in [60]. The reduced inverter rating for voltage and frequency control for SEIG is also suggested [61]. Another control algorithms based on leaky minimal disturbance theory (LMDT) for enhance power generation with controlled voltage and frequency is proposed [62]. The constant voltage and frequency operation of SEIG has been analyzed in steady state condition using Genetic Algorithm [63]. An optimized operation is achieved for power quality improvement using Antlion Algorithm [64]. The AC/DC Hybrid system is developed using dual stator winding generator with static excitation controller [65]. There are controllers proposed for voltage and frequency control using electronic load controller and generalized impedance controller [66-68]. The series compensation-based scheme is for frequency sensitive loads [69]. For isolated power generation system with high wind penetration a frequency control scheme is discussed [70]. A dynamic VAR control scheme in wind turbine generators is discussed for mitigation of flickers [71]. A micro-controller for voltage and frequency control, flicker etc in case of wind turbine-based system is described and adaptation of control system is also reported [72]. The controller which is based on intelligent neural network has been implemented for wind energy conversion system [73]. A recurrent fuzzy neural network has been used in a three-phase SEIG-based system [74]. A power electronic converter is used for excitation of an induction generator [75]. The

controller used have the same reactive power rating as that of induction generator. The main advantage for such kind of excitation is to remove the excitation of generator in discrete steps which may be higher or lower than required excitation.

## **1.7 Advantages and Novelties of Proposed Control**

The few interesting features of the anticipated control techniques are mentioned below:

1. The proposed control schemes of VSC for SEIG system improve the adaptation performance instead of its current values.
2. In proposed control techniques, the quantity of earlier gradients is used for updating the present and hence gives more precise and faster convergent results.
3. It gives the faster convergent rate and minimum probability of trapping in the local minima, in the proposed distributed generation system for control of voltage and frequency in a three-phase SEIG.
4. It provides faster dynamics in voltage and frequency control either variation in wind speed or random variations in loads. The implementation of algorithm named Leaky-Momentum Control Algorithm (LMA) is discussed and analyzed in details.
5. A modified NLMS control has been also implemented to estimate the fundamental load current component and generate the triggering pulses for VSC.
6. A modified NLMS control with VSC provides rapid convergence, harmonic eradication, fast dynamic response with reduced oscillations, load leveling, compensation of neutral current and enhance the power quality in standalone SEIG system operation.
7. A BES is being interfaced at DC link of VSC which is employed to provide active power support between the SEIG and the load under dynamic conditions of wind and loads.

## 1.8 Organization of Thesis

The work presented in this thesis is divided into six chapters excluding abstract and acknowledgement.

The Chapter-I presents introduction and the state of art literature review on voltage and frequency control methods and algorithms for SEIG. In this chapter, extensive literature survey is carried out and findings are cited.

The Chapter-II presents research objectives and methodology. In this chapter, objectives are derived for the research work to be carried out. Moreover, systematic planning and approaches are discussed to achieve the desired research objectives.

The Chapter-III presents configuration of proposed SEIG system and estimation of capacitors required to excite and operate the self-excited induction generator under steady state condition.

The various techniques for estimation of capacitor are provided in this chapter.

The Chapter-IV presents implementation of Leaky momentum control algorithm to improve the power quality issues in standalone such as voltage and frequency variation under varying load conditions, harmonics mitigation in the source current and reactive power compensation etc. The control algorithm modelling, simulation results and experimental demonstration of proposed scheme are also discussed.

The Chapter-V presents implementation of a new control algorithm (Modified NLMS) for maintaining terminal voltage and frequency under varying wind speed and load conditions for a standalone SEIG system.

The Chapter-VI presents conclusion and future scope of the present work and in last section of the thesis, the appendix, list of publications, author's biography and references are provided.

## **CHAPTER 2**

### **RESEARCH OBJECTIVES AND METHODOLOGY**

---

#### **2.1 General**

The chapter 1 of this thesis covered the detailed literature study in the domain of voltage and frequency control of self-excited induction generator. Moreover, study on control algorithms which are most suitable for power quality improvement of SEIG, have been major focused area of the present research work. The suitability of control algorithm should be based on accuracy, faster dynamic response and less steady state error under variable wind speed or varying load conditions in wind energy-based operation of SEIG. An extensive literature review of the published research work is carried out and accordingly research objectives are devised.

#### **2.2 Research Objectives of the Thesis**

1. Power quality improvement in VSC based operation of three phase self-excited induction generator using advanced control algorithms as per IEEE -519 standards under variable speed operation and varying load conditions.
2. Voltage and frequency control of self-excited induction generator in variable speed wind energy conversion system under varying load conditions.

#### **2.3 Major Contributions**

The main contributions in this thesis are as follows:

1. Planning and Development of three phase self-excited induction generator-based generation system for supplying power to isolated locations.
2. To design the control algorithm for power quality improvement including voltage and frequency control of SEIG under varying loads.



3. To evolve applications of new control algorithms for operation of VSC based control of SEIG and implementation of the control scheme in MATLAB/Simulink for validation of their performance.
4. To develop prototype experimental study set-up for validation of adopted control algorithms for power quality improvement of SEIG system.

## **2.4 Research Methodology**

The research methodology consists of generation system planning, designing of control algorithms, simulation study in MATLAB/Simulink and hardware experimentation to validate the proposed research objectives.

### **2.4.1 Planning of SEIG based Standalone Generation System**

The complete system is planned and designed as per the loading requirements for standalone operation of SEIG. The rating of SEIG is selected accordingly to a specified load and battery energy storage system. The rating of wind turbine is estimated for driving the SEIG. A VSC is connected at point of common coupling (PCC), accordingly rating of VSC is also evaluated. Due to isolated operation of the SEIG system, a battery back-up is also needed to support the SEIG and load under varying load conditions. An integrated operation of all the units is planned for ensuring power quality index as per IEEE-519 standard. The equipment ratings are given in appendix.

### **2.4.2 Design of Control Algorithms**

The reference source current to operate the VSC is estimated with the use of control algorithm. Three phase reference source currents are utilized by PWM technique to generate the gate pulses for six Insulated Gate Bipolar Transistors (IGBTs) of VSC. The PWM voltage output of VSC injects current at PCC for compensation of the load current. The injected currents at PCC are such that only fundamental current component of load is to be supplied from the generator terminals, other multiple frequency current harmonics components are

supplied from the VSC. For faster load dynamics, execution speed of the control scheme should be fast enough to catch the dynamics of the load current. Therefore, fast, accurate and adaptive response are the required features of any control algorithm used for reference generation. Many control algorithms based on adaptive control theory have been published in literature for STATCOM or shunt active power filters. In the present work, some new adaptive control algorithms have been implemented for VSC control to improve power quality issues in SEIG based wind energy conversion system for isolated applications.

#### **2.4.3 To perform the MATLAB Simulations**

The generation system model has been developed using MATLAB/Simulink library toolboxes and simulations are carried out in a discrete mode with a variable step size and an ode23tb (stiff / TR-BDF-2) solver. The system power circuit and control circuit diagram are built and properly interfaced for simulation study. The waveforms of various electrical quantities of interest are captured and analyzed for verifying the research objectives.

#### **2.4.4 To perform the Experimentation**

The laboratory prototype of the proposed system is developed for experimentation where SEIG is major component for power generation and dSPACE-1104 is working as a controller. The diode based non-linear consumer loads are used for VSC performance assessment. The Hall-effect voltage sensors are used to sense ac phase voltages and dc link voltage of VSC. The Hall-effect current sensors are also used to sense various currents at PCC. The DS 1104 R&D controller is used to generate the gate pulses for IGBTs of VSC. The gate pulses are fed to three-leg IGBT module and control algorithm is run inside the processor.

### **2.5 Conclusions**

This chapter is summarized as below:

- (a) Research objectives are derived for the present work in thesis.
- (b) The detail planning and methodology to fulfill the research objectives are discussed.

(c) The components of simulation tools and hardware prototype have also been discussed.

## CHAPTER 3

# SEIG CONFIGURATION FOR DISTRIBUTED GENERATION AND ESTIMATION OF EXCITATION CAPACITANCE

---

### 3.1 General

Conventional sources of energy such as fossil fuels are not environmentally friendly and continuously depleting. The adverse effects of conventional energy sources may be prevented by means of using renewable energy sources such as wind, solar, hydro and tidal energy, etc. Self-excited induction generators have gained importance in recent years owing to the global trend towards usage of wind energy, which is renewable and cleaner sources of energy. SEIGs are robust in design, have long life, require minimal maintenance and able to generate power at varying speed. They find application in wind energy conversion system for harnessing wind energy. The system under study in this chapter is a wind turbine coupled self-excited induction generator, delivering power to a three-phase balanced load, with an excitation capacitor bank. For standalone operation with varying speed a minimum capacitance is required to maintain self-excitation of SEIG. An analysis of this SEIG system is carried out for variable speed applications by solving the non-linear algebraic equations governing the performance of the system in steady state condition. Multivariate Newton Raphson technique has been employed for obtaining the solution of algebraic equation, where excitation reactance ( $X_c$ ) and per unit speed ( $N$ ) are chosen as variables and allowed to vary within their upper and lower bounds. Thereby a study is being carried out on the speed and minimum excitation capacitor requirement for generation of rated voltage under varying load conditions.

### 3.2 `SEIG System Configuration

A basic SEIG configuration with shunt excitation capacitor bank is considered for analysis in the present work for wind energy applications. Fig. 3.1 shows the wind turbine driven SEIG system supplying isolated loads. A capacitor bank is interfaced at the terminal of SEIG to generate rated voltage. The steady state performance of SEIG is analyzed under varying wind velocity and varying load demand.

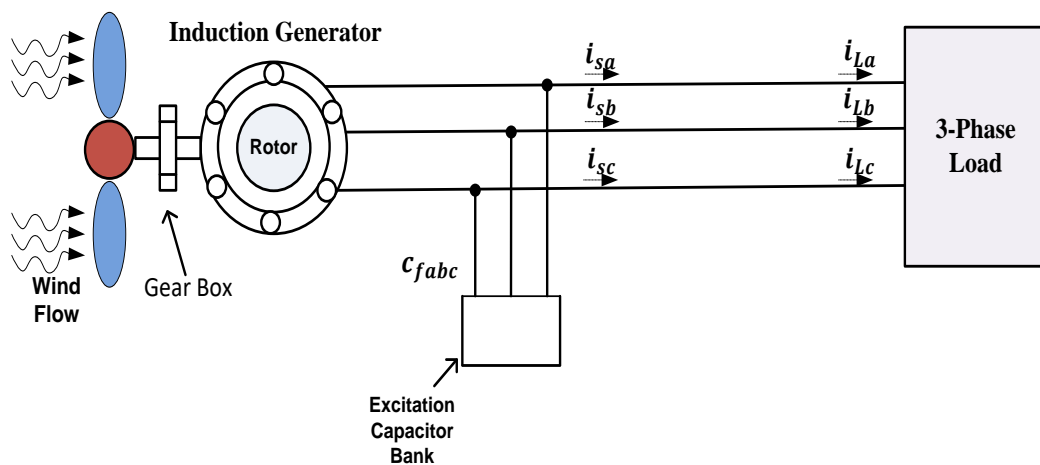


Fig. 3.1 A SEIG coupled to a wind turbine and delivering power to a 3 phase load

### 3.3 Method for determining Excitation Capacitance for rated voltage operation of SEIG under varying Loads.

Rising demand for energy is a consequence of rapid development happening all around the world. Proportion of power which is generated through conventional sources, like coal, fuel and gas, is around 70-75% of the total generation, which causes harmful effects on environment. Thus, in recent years emphasis has been laid for use of non-conventional energy sources for power generation like: solar, wind, hydro, bio-gas etc. Among these renewable sources it has been found that wind is one of the most potential resources for electricity generation [76-78]. Induction generator is popularly employed for harnessing wind energy because of its capability to generate power at variable speeds. It has advantages like low cost, small size, robust design, and minimal maintenance and repair [79]. Induction generator has an

important feature of self-excitation, which is possible by connecting a capacitor bank across the stator terminal of the induction generator. The self-excitation process in SEIG is similar to that observed in dc generator. Also, there should be some residual magnetism present in machine, which is essential to initiate the voltage build up process in SEIG. Also, it is noted that the residual magnetism must be enough for voltage build up process to occur. T. F. Chan et.al [80] described a practical approach to compute the minimum values of capacitance required for initiation of voltage build-up process in a three-phase SEIG. Despite its numerous advantages SEIG finds limited applications due to its poor voltage and frequency regulation. However, introduction of power electronic controllers has significantly changed the scenario of its potential applications in distributed generation. Venkatesa and Singh have examined the performance of SEIG using controllers like impedance controller and DSTATCOM [81-82] and it was demonstrated that these controllers are quite effective in regulating output voltage and frequency. The frequency and voltage control issues of a three-phase SEIG-based distributed generating system were analysed [83] and the Leaky-momentum control technique is implemented to control the voltage -source converter in wind energy conversion system using SEIG. For studying the power generation and problems associated with SIEG using wind energy, steady state analysis of SEIG is necessary under varying speed and load conditions. There are various methods for steady state analysis, the most common being application of loop impedance and nodal admittance method for per phase equivalent electrical circuit of the SEIG. Steady state analysis of SEIG has been examined and presented by S.S. Murthy [84] and Sharad Rajan [85]. In this paper nodal admittance method has been used for obtaining the non-linear equations governing the system in steady state. These non-linear equations are used in study and analysis of performance parameters such as output power, value of excitation capacitance, speed and generated voltage and frequency.

In previous published work on performance analysis of SEIG, magnetizing reactance ( $X_m$ ) of machine and frequency (f) of generated voltage has been evaluated for known values of load, speed and capacitor bank. D.K. Jain, et al. [86] developed a new iterative technique for steady state analysis of a three phase SEIG, thereby determining the frequency and magnetizing reactance. A similar work is presented using linear search and binary search algorithms [87]. Applications of optimization techniques GA, APSO, PSO and simulated annealing for steady state analysis of SEIG has also been reported in literatures [88-89].

However, in the analysis presented in this chapter, the value of magnetizing reactance is fixed for rated voltage operation and the generated frequency as 50 Hz in all the nonlinear algebraic equations which are governing the system in steady state condition. The nonlinear algebraic equations are solved for the value of capacitance to be connected at stator terminal and the corresponding rotor speed for different types of loads to maintain self-excitation in the machine. Multivariate Newton-Raphson technique is used to obtain the solution of these nonlinear algebraic equations. Once speed and capacitance are known, evaluation of load voltage, load current and output power is obtained.

### **3.3.1 Steady state Analysis of SEIG**

Fig. 3.1 represents the schematic diagram of SEIG setup under study for estimation of capacitance. A wind turbine is coupled, via gear, to the rotor of an induction generator. A capacitor bank is connected at stator terminals for providing reactive power support to generator and load.

Per phase equivalent circuit of the SEIG is shown in Fig 3.2

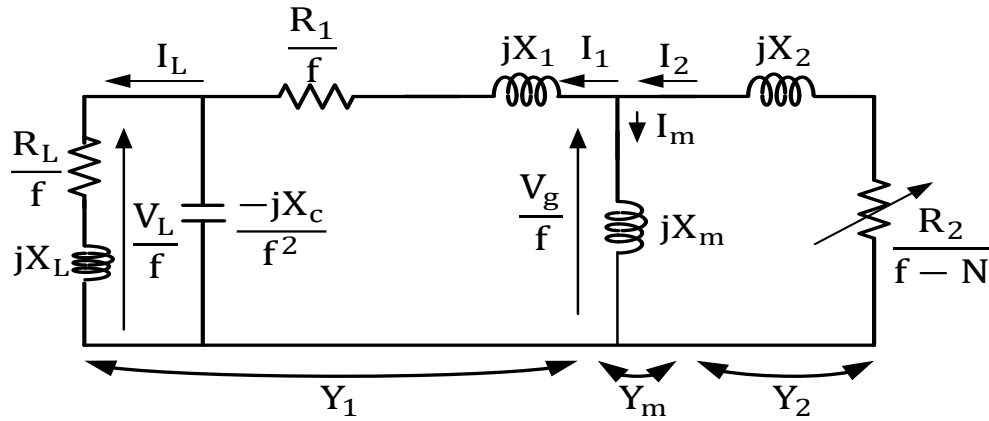


Fig. 3.2 Per phase equivalent circuit of SEIG

Where

$R_1$ : Stator Resistance

$R_2$ : Rotor Resistance (referred to stator)

$X_1$ : Stator Leakage Reactance

$X_2$ : Rotor Leakage Reactance (referred to stator)

$X_m$ : Magnetizing Reactance

$X_c$ : Excitation Capacitive Reactance

$R_L$ : Load Resistance

$X_L$ : Load Reactance

$f$ : Per unit frequency

$N$ : Per unit speed

Application of KCL in the equivalent circuit yields

$$I_1 + I_m = I_2 \quad (3.1)$$

$$\frac{V_g}{f} \times Y_1 + \frac{V_g}{f} \times Y_m = -\frac{V_g}{f} \times Y_2 \quad (3.2)$$

Since air gap voltage must not be zero i.e.,  $V_g \neq 0$ , Therefore

$$Y_1 + Y_2 + Y_m = 0 \quad (3.3)$$



Where

$$Y_1 = \frac{1}{\left(\frac{R_1}{f} + jX_1\right) + (R - jX)} \quad (3.4)$$

$$R - jX = \frac{\left(\frac{R_L}{f} + jX_L\right) \times \left(\frac{-jX_C}{f^2}\right)}{\frac{R_L}{f} + j\left(X_L - \frac{X_C}{f^2}\right)} \quad (3.5)$$

$$R = \frac{\left(\frac{R_L}{f}\right)(X_L)\left(\frac{X_C}{f^2}\right) - \left(\frac{R_L}{f}\right)\left(\frac{X_C}{f^2}\right)\left(X_L - \frac{X_C}{f^2}\right)}{\left(\frac{R_L}{f}\right)^2 + \left(X_L - \frac{X_C}{f^2}\right)^2} \quad (3.6)$$

$$X = \frac{(X_L)\left(\frac{X_C}{f^2}\right)\left(X_L - \frac{X_C}{f^2}\right) + \left(\frac{R_L}{f}\right)^2\left(\frac{X_C}{f^2}\right)}{\left(\frac{R_L}{f}\right)^2 + \left(X_L - \frac{X_C}{f^2}\right)^2} \quad (3.7)$$

$$Y_m = \frac{-j}{X_m} \quad (3.8)$$

$$Y_2 = \frac{1}{\frac{R_2}{f-N} + jX_2} \quad (3.9)$$

Equating real and imaginary parts of equation (3.3) to zero, real part yields

$$\frac{\left(R + \frac{R_1}{f}\right)}{\left(R + \frac{R_1}{f}\right)^2 + (X_1 - X)^2} + \frac{\left(\frac{R_2}{f-N}\right)}{\left(\frac{R_2}{f-N}\right)^2 + (X_2)^2} = 0 \quad (3.10)$$

and equating imaginary part

$$\frac{(X_1 - X)}{\left(R + \frac{R_1}{f}\right)^2 + (X_1 - X)^2} + \frac{(X_2)}{\left(\frac{R_2}{f-N}\right)^2 + (X_2)^2} + \frac{1}{X_m} = 0 \quad (3.11)$$

### 3.3.2 Performance analysis using Multivariate Newton-Raphson Method

Equations (3.10) and (3.11) have been solved for known values of speed, load and excitation capacitance. Solution of these equations thus yields value of generated frequency & magnetizing reactance. However, in the present analysis, aim is to evaluate the speed and capacitance required for rated voltage operation of a SEIG, i.e., at rated value of  $X_m$  and rated frequency which is 50 Hz and parameters load voltage, current and power are evaluated.

Once  $X_m$  and  $f$  are fixed, and considering the applied load to be balanced, each of equations (3.10) and (3.11) is essentially a two variable function given by:

$$Re(Y) = F_1(X_C, N) = \frac{\left(R + \frac{R_1}{f}\right)}{\left(R + \frac{R_1}{f}\right)^2 + (X_1 - X)^2} + \frac{\left(\frac{R_2}{f - N}\right)}{\left(\frac{R_2}{f - N}\right)^2 + (X_2)^2} = 0 \quad (3.12)$$

$$Im(Y) = F_2(X_C, N) = \frac{(X_1 - X)}{\left(R + \frac{R_1}{f}\right)^2 + (X_1 - X)^2} + \frac{(X_2)}{\left(\frac{R_2}{f - N}\right)^2 + (X_2)^2} + \frac{1}{X_m} = 0 \quad (3.13)$$

There are two nonlinear equations with two unknowns: the excitation capacitive reactance ( $X_C$ ) and the per unit speed ( $N$ ). The equations (3.12) and (3.13) are solved for  $X_C$  and  $N$  using the Multivariate Newton Raphson Method given below:

$$X^{i+1} = X^i - [J^i]^{-1} F^i \quad (3.14)$$

Where,  $X^i$ ,  $J^i$  and  $F^i$  are given by equations (3.15), (3.16) and (3.17) respectively.

$$X^i = \begin{bmatrix} X_C^i \\ N^i \end{bmatrix} \quad (3.15)$$

$$J^i = \begin{bmatrix} \left. \frac{\partial F_1(X_C, N)}{\partial X_C} \right|_{(X_C^i, N^i)} & \left. \frac{\partial F_1(X_C, N)}{\partial N} \right|_{(X_C^i, N^i)} \\ \left. \frac{\partial F_2(X_C, N)}{\partial X_C} \right|_{(X_C^i, N^i)} & \left. \frac{\partial F_2(X_C, N)}{\partial N} \right|_{(X_C^i, N^i)} \end{bmatrix} \quad (3.16)$$

$$F^i = \begin{bmatrix} F_1(X_C^i, N^i) \\ F_2(X_C^i, N^i) \end{bmatrix} \quad (3.17)$$

Initially  $i=0$  and  $X^0$  is the initial solution guess, and thereby  $X^1$  is evaluated with help of equation (3.14). Each iteration of equation (3.14) gives a closer value to the actual solution. Hence, similarly  $X^2$  is evaluated after having found  $X^1$ , and so on  $X^3$ ,  $X^4$  ... are evaluated. Equation (3.14) is allowed to execute in a loop and the condition for the termination of loop is when the solution, i.e.,  $X_C$  and  $N$ , either starts repeating itself or converges. Once  $X_C$  and  $N$  are known, capacitance is simply given by equation (3.18)

$$C = \frac{1}{2 \times \pi \times 50 \times X_C} \quad (3.18)$$

and rotor speed is given by equation (3.19)

$$N_r = N \times \text{synchronous speed} \quad (3.19)$$

Load voltage and current are obtained using equations (3.20) and (3.21) respectively. Equation (3.22) and (3.23) are used for calculating power.

$$V_L = \frac{\sqrt{R^2 + X^2}}{\sqrt{\left(R + \frac{R_1}{f}\right)^2 + (X_1 - X)^2}} \times V_g \quad (3.20)$$

$$I_L = \sqrt{3} \times \frac{\frac{V_L}{f}}{\sqrt{\left(\frac{R_L}{f}\right)^2 + (X_L)^2}} \quad (3.21)$$

$$\text{Output Power (in kVA)} = \frac{\sqrt{3} \times V_L \times I_L}{1000} \quad (3.22)$$

$$\text{Output Power (in kW)} = \frac{\sqrt{3} \times V_L \times I_L \times \cos(\theta)}{1000} \quad (3.23)$$

### 3.4 Results and Discussions

Induction machine considered for the present study is rated as 3.7 kW, 3 Phase, 4 Pole, 50 Hz, 415 V, 7.6 A, 1420 rpm. Also, per phase stator and rotor parameters of the machine are  $R_1 = 0.053$  p.u,  $R_2 = 0.061$  p.u,  $X_1 = 0.087$  p.u,  $X_2 = 0.087$  p.u, and magnetizing reactance  $X_m = 1.853$  p.u.

In equations (3.12) and (3.13), values of  $f$  and  $X_m$  are taken as 1 p.u and 1.853 p.u. respectively. Multivariate Newton Raphson method is applied, as discussed in section 3, to solve for ' $X_C$ ' and ' $N$ '. Two different types of balanced loads are considered for present study: purely resistive load ( $\text{pf} = 1$ ) and inductive load ( $\text{pf} = 0.8$  lagging).

Varying resistive loads, of per phase value, 1 p.u, 1.2 p.u, 1.4 p.u, 1.6 p.u, 1.8 p.u and 2 p.u are considered at the stator terminals at rated voltage condition. The values of speed and capacitance requirements for rated operation are predetermined using Newton Raphson technique with varying loads. Load voltage, line current and three phase output power have been determined and shown in table 3.1.

Table 3.1. Self-excitation capacitance requirements under varying resistive loads

S no.	R <sub>L</sub> (p.u)	Speed (rpm)	Slip (%)	Excitation Capacitance per phase (μF)	V <sub>L</sub> (V)	I <sub>L</sub> (A)	Power(kW)
1	1.0	1601.5	-6.7652	26.156	417.6335	7.6490	5.530
2	1.2	1584.4	-5.6250	23.672	419.5780	6.4038	4.654
3	1.4	1572.4	-4.8248	22.171	421.1734	5.5099	4.019
4	1.6	1563.4	-4.2301	21.184	422.4807	4.8361	3.539
5	1.8	1556.6	-3.7699	20.498	423.5628	4.3098	3.162
6	2.0	1551.0	-3.4027	19.997	424.4696	3.8871	2.858

Output Load voltages obtained for various upf loads are very close to rated voltage, as shown in Fig. 3.3 and hence voltage of the SEIG is regulated within the permissible limit with varying requirements of excitation capacitors. Also, it is noted that all the output voltages are determined/calculated at rated frequency i.e., 50 Hz and at upf loads. It is observed that with almost 100% increase of load currents (3.889 A to 7.649 A), the terminal voltage of generator changes only from 424 V to 417 V.

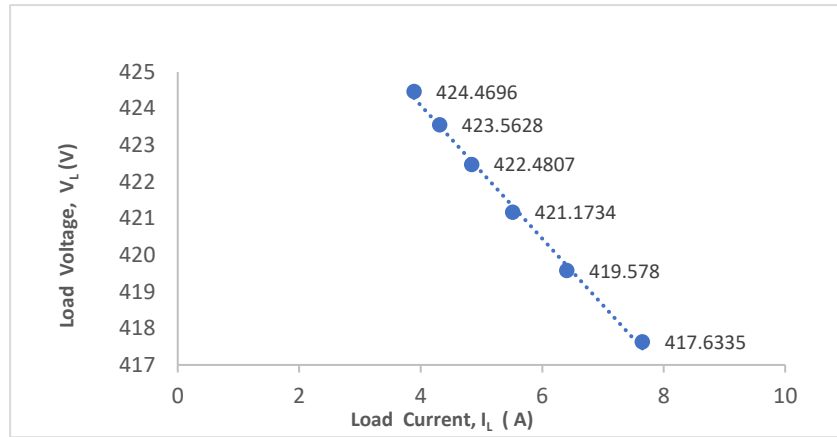


Fig. 3.3 Variation of load voltage with load current of SEIG at resistive loads.

This analysis is also carried out for inductive loads at 0.8 lagging pf. The load Impedance connected at the stator terminal is varied in steps as 1.25 p.u, 1.375 p.u, 1.5 p.u, 1.625 p.u, 1.75 p.u and 1.875 p.u. The steady state performance with inductive loads is also analyzed using modified Newton Raphson technique and are shown in table 3.2. and it is observed that with 50% increase of load currents (from 4.1585 A to 6.1869 A) the terminal voltages fall only from 425 V to 422 V.

Table 3.2 Excitation capacitance requirements under varying inductive loads (0.8 pf lagging)

S no.	$Z_L$ (p.u)	Speed (rpm)	Slip (%)	Excitation Capacitance per phase ( $\mu$ F)	$V_L$ (V)	$I_L$ (A)	Power	
							kVA	kW
1	1.250	1564.947	-4.3298	37.498	422.2545	6.1869	4.52	3.62
2	1.375	1559.156	-3.9438	35.434	423.1468	5.6363	4.13	3.30
3	1.500	1554.344	-3.6229	33.756	423.9211	5.1761	3.80	3.04
4	1.625	1550.279	-3.3519	32.359	424.5980	4.7856	3.52	2.82
5	1.750	1546.799	-3.1199	31.181	425.1943	4.4500	3.28	2.62
6	1.875	1543.784	-2.9189	30.173	425.7230	4.1585	3.07	2.45

Fig 3.4 shows the variation of output terminal voltages of SEIG at rated frequency 50Hz with the increase of load current at inductive load of 0.8 pf. It is observed that with increase of load, the terminal voltage of generator falls from 425 V to 422 V at rated frequency 50 Hz.

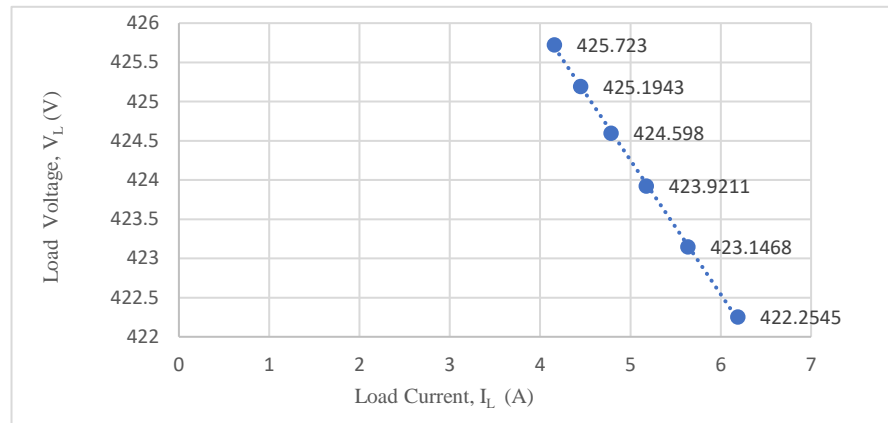


Fig 3.4 Output voltages versus load current under varying inductive loads.

### 3.5 Conclusion

In this chapter a simple approach to determine the capacitance and rotor speed, for different load conditions of SEIG, which ensures rated operation of a SEIG is presented. It is inferred that for varying resistive loads for different speed, there is a minimum excitation capacitance requirement to maintain self-excitation in the machine and maintain operation at rated voltage. Similar trend is observed when inductive loads (0.8 pf lagging) ranging between 1.250 p.u – 1.875 p.u are considered. Again, with increasing load current, the excitation capacitance requirement increases and terminal voltage is maintained near to rated voltage. Frequency of generated voltage is 50 Hz in all cases. It is noted that load power is compromised for ensuring rated voltage operation under inductive load. The present analysis is helpful in designing of power electronics-based controller which constantly monitors the load and for any change in load current it automatically generates needed reactive power compensation to the SEIG to maintain rated output voltage and frequency.

## CHAPTER 4

# IMPLEMENTATION OF LEAKY-MOMENTUM CONTROL ALGORITHM FOR VOLTAGE AND FREQUENCY CONTROL OF 3-PHASE SEIG

### 4.1 General

This chapter presents implementation of Leaky-Momentum Algorithm (LMA) based control scheme used for switching control of VSC for regulation of voltage and frequency in SEIG based distributed generation system, power balancing and other power quality issues such as harmonic compensation and neutral current compensation under varying load conditions. The schematic diagram of the SEIG based distributed generation system with the proposed LMA control algorithm is shown in Fig. 4.1.

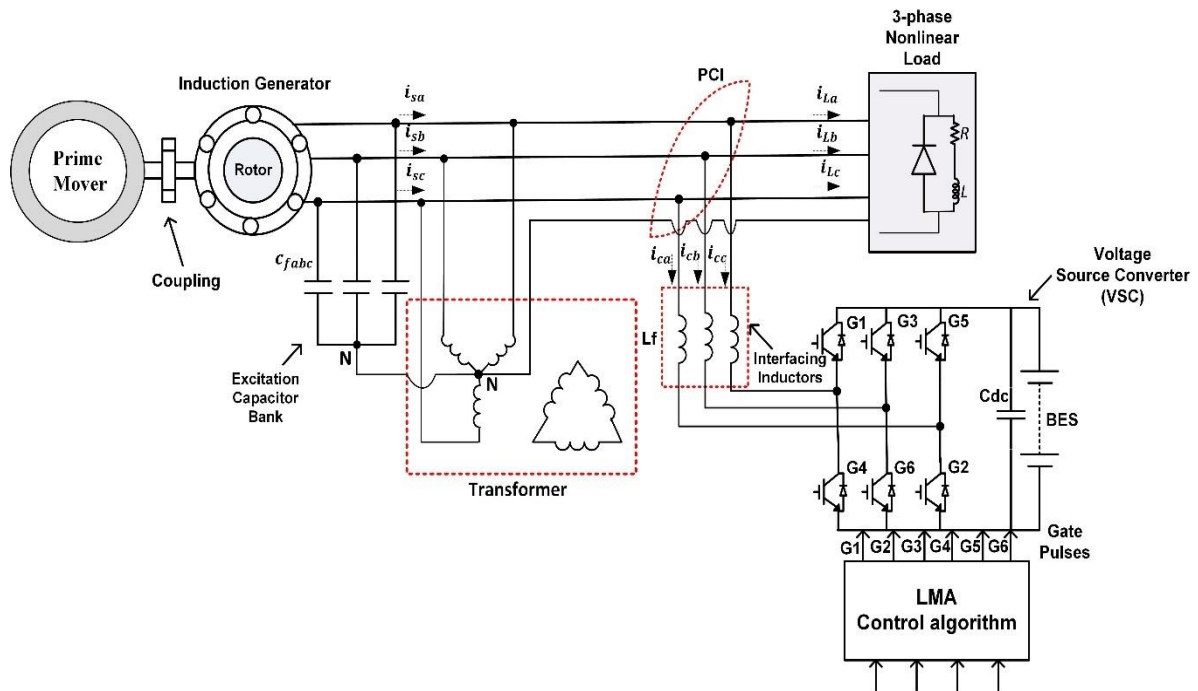


Fig. 4.1 Schematic diagram of distributed generation (DG) system based on LMA control algorithm.

A three-phase star-connected variable capacitor bank is interfaced at the terminal of SEIG to generate rated voltage at no load. A three-phase star-delta (Y- $\Delta$ ) transformer is being used for

neutral current compensation under unbalanced load conditions. The neutral points of capacitor bank, transformer and load are connected to a common point. A DSTATCOM is interfaced in shunt at the point of common interface (PCI) through interfacing inductors. The battery energy storage system (BES) is interfaced at DC link and consumes the extra power under less load condition. The procedure for reference current estimation is elaborated below which is used to generate the switching pulses of voltage source converter.

The simulation model of three-phase induction generator is developed in MATLAB with a VSC and nonlinear load and simulation is carried out under various operating conditions to analyze the performance of SEIG system using LMA control scheme of VSC. The developed LMA control Algorithm has been executed for generating control signals for VSC and regulating the voltage and frequency of proposed system. This control technique has been used to calculate the updated weights of load current components and after finding these weights, reference source currents components are computed. For mitigation of power quality problems in standalone wind energy system using SEIG, the adequate ratings of DSTATCOM and BES are selected.

## **4.2 Leaky Momentum Control Algorithm: An Introduction**

Applications of adaptive filtering in control of VSC have grown significantly in the last few decades. The least mean square algorithm (LMS) has become one of the most popular adaptive filtering algorithms due to its inherent simplicity and robustness but it often converges slowly. Further LMS and its variant such as normalized LMS or modified LMS (MLMS) do not perform well in noisy or distorted signal conditions. This section analyses the leaky momentum LMS algorithm which provides information regarding the almost sure behavior of the parameter estimates due to its flexible convergence property and it offers an improvement in convergence rate as compared to that of LMS. The leaky momentum control algorithm is implemented for the extraction of reference current from the estimated values of active and



reactive components of distorted or nonlinear load current to operate the shunt connected voltage source converter. Due to decreasing spread of input Eigen values, the faster convergence is achieved under variable input output operating conditions. Moreover, the dynamic response of voltage source converter is also improved for various operating conditions. The value of the leaky factor and momentum factor must be between 0 to 1, and most of the time it should be near to 1 to reduce the Eigen spread for the simultaneously improved dynamic response.

In any linear system, its input  $u(n)$  and output  $x(n)$  is normally related by

$$x(n) = h^T u(n) + d(n) \quad (4.1)$$

Where  $h$  is the impulse response of the system with  $L$  tap length,  $u(n)$  is the input tap vector in linear system and  $d(n)$  is the distortion or independent surplus noise.

The objective function that can be minimized by leaky momentum algorithm is as follows

$$J(n) = e^2(n) + \gamma z^T(n)z(n) \quad (4.2)$$

where  $z(n)$  is the weight coefficient vector of the adaptive algorithm with length  $L$ ,  $\gamma$  is known as leakage factor which is a positive and  $e(n)$  is the error signal given by

$$e(n) = x(n) - z^T(n) u(n) \quad (4.3)$$

The minimum of  $J(n)$  can be sought recursively using the gradient method [40]

$$\begin{aligned} z(n+1) &= z(n) - \mu (\partial J(n) / \partial z(n)) \\ &= (1 - \mu \gamma) z(n) + \mu e(n) u(n) + \alpha [z(n) - z(n-1)] \end{aligned} \quad (4.4)$$

where  $\mu$  is the size of adaptation step and  $\alpha$  is momentum factor [90],[91]. This equation is finally utilized to achieve the reference current for voltage source converter. This is convergent equation and gives the optimum value of weight throughout tap length.

#### 4.2.1 Weight calculation using LMA Control Algorithm

Peak value of terminal voltage ( $V_t$ ) of SEIG is calculated using sensed 3-phase terminal voltage of the SEIG.

$$V_t = \sqrt{2 \left( \frac{v_{sa}^2 + v_{sb}^2 + v_{sc}^2}{3} \right)} \quad (4.5)$$

$v_{sa}$ ,  $v_{sb}$  and  $v_{sc}$  represents instantaneous phase voltages at PCI. The in-phase unit voltage templates are calculated as follows:

$$u_{pa} = \frac{v_{sa}}{V_t}, \quad u_{pb} = \frac{v_{sb}}{V_t}, \quad u_{pc} = \frac{v_{sc}}{V_t} \quad (4.6)$$

$$\begin{bmatrix} u_{qa} \\ u_{qb} \\ u_{qc} \end{bmatrix} = \frac{1}{\sqrt{3}} \begin{bmatrix} -1 & 0 & 1 \\ \sqrt{3} & 1 & -1 \\ -\sqrt{3} & \frac{1}{2} & -\frac{1}{2} \end{bmatrix} \begin{bmatrix} u_{pa} \\ u_{pb} \\ u_{pc} \end{bmatrix} \quad (4.7)$$

Where  $u_{pa}$ ,  $u_{pb}$  and  $u_{pc}$  shows unit voltages template of in-phase component respectively.

All unit voltages are instantaneous phase voltages. Similarly,  $u_{qa}$ ,  $u_{qb}$  and  $u_{qc}$  are the quadrature phase instantaneous unit voltage templates of 3- phase voltages.

A Leaky Momentum Control Algorithm is used to update the weights of active ( $w_{pa}$ ) and reactive ( $w_{qa}$ ) components of the fundamental load current. Here, the weights are adjusted till the error in the current state and previous state becomes zero. The active component of power of phase a load current is estimated as shown below:

$$w_{pa}(n+1) = (1 - \tau_p \alpha) w_{pa}(n) + \tau_p u_{pa}(n) e_{pa}(n) - u_{pa}(n) e_{npa}(n) + \varepsilon (w_{pa}(n) - w_{pa}(n-1)) \quad (4.8)$$

Where,  $e_{pa}(n)$  and  $e_{npa}(n)$  are the adaptive error component and noise component of the proposed control algorithm for phase 'a'.

The following equations are used to determine the relation between both factors:

$$e_{pa}(n) = w_{sp}(n-1) - \{(1 - \tau_p \alpha) w_{Lpavg}(n-1) u_{pa}(n-1)\} - \tau_p \{\sigma e_{pa}(n-1) i_{La}(n-1) u_{pa}(n-1)\} \quad (4.9)$$

and

$$e_{npa}(n-1) = k u_{pa}(n) \{w_{pa}(n) - w_{sp}(n)\} \quad (4.10)$$

Where,  $w_{Lpavg}(n-1)$  is average amplitude of active power component of load current,  $w_{sp}(n-1)$  is the total active components of reference supply currents and  $i_{La}(n-1)$  is load current of phase 'a' at  $(n-1)^{th}$  sampling instant. Other factors  $k$ ,  $\alpha$ ,  $\sigma$  and  $\tau_p$  are noise factor, leaky factor, error constant factor and learning rate respectively.

Similarly, for active power components of phase b and phase c are estimated as follows:

$$w_{pb}(n+1) = (1-\tau_p\alpha) w_{pb}(n) + \tau_p u_{pb}(n) e_{pb}(n) - u_{pb}(n) e_{npb}(n) + \varepsilon(w_{pb}(n) - w_{pb}(n-1)) \quad (4.11)$$

$$w_{pc}(n+1) = (1-\tau_p\alpha) w_{pc}(n) + \tau_p u_{pc}(n) e_{pc}(n) - u_{pc}(n) e_{npc}(n) + \varepsilon(w_{pc}(n) - w_{pc}(n-1)) \quad (4.12)$$

The average magnitude of weighted fundamental active power components is calculated by

$$w_{Lpavg} = \frac{(w_{pa} + w_{pb} + w_{pc})}{3} \quad (4.13)$$

In the similar manner as estimated in above mentioned equations, reactive components of the three-phase (a, b, c) load currents can be estimated as follows:

$$w_{qa}(n+1) = (1-\tau_q\alpha) w_{qa}(n) + \tau_q u_{qa}(n) e_{qa}(n) - u_{qa}(n) e_{nqa}(n) + \varepsilon(w_{qa}(n) - w_{qa}(n-1)) \quad (4.14)$$

$$w_{qb}(n+1) = (1-\tau_q\alpha) w_{qb}(n) + \tau_q u_{qb}(n) e_{qb}(n) - u_{qb}(n) e_{nqb}(n) + \varepsilon(w_{qb}(n) - w_{qb}(n-1)) \quad (4.15)$$

$$w_{qc}(n+1) = (1-\tau_q\alpha) w_{qc}(n) + \tau_q u_{qc}(n) e_{qc}(n) - u_{qc}(n) e_{nqc}(n) + \varepsilon(w_{qc}(n) - w_{qc}(n-1)) \quad (4.16)$$

Where,  $\tau_q$  is the learning rate of proposed control algorithm for reactive power component estimation.

The average magnitude of weighted fundamental reactive ( $w_{Lqavg}$ ) power components is calculated by

$$w_{Lqavg} = \frac{(w_{qa} + w_{qb} + w_{qc})}{3} \quad (4.17)$$

#### 4.2.2 Reference Source current calculation and gate pulses generation

Reference source current is obtained by adding active and reactive components of source current obtained as below.

$$i_{sabc}^* = i_{spt}^* + i_{sqt}^* \quad (4.18)$$

The source current  $i_{sabc}$  is sensed and this estimated reference current  $i_{sabc}^*$  are given at the input to the hysteresis current controller for generation of gate pulses. The complete LMA control process is shown in control diagram of the system in Fig. 4.2

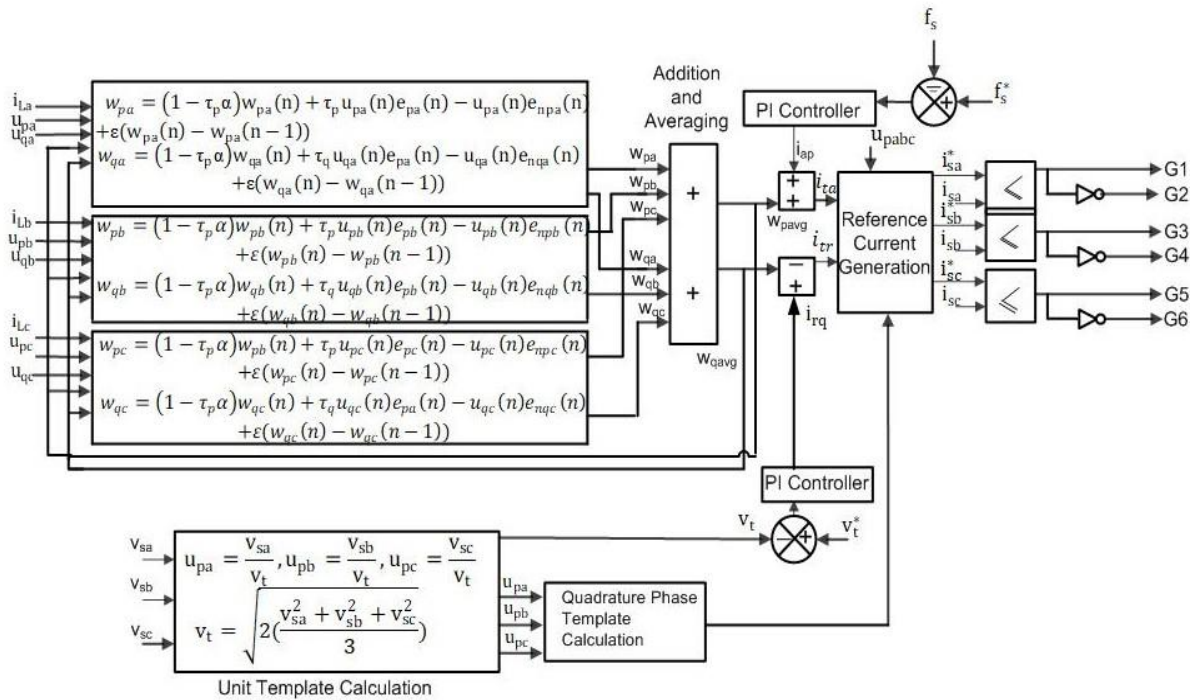


Fig. 4.2 Block Diagram of LMA control Algorithm

### 4.3 Simulation Results of SEIG Based Distributed Generation using Leaky Momentum Control Algorithm

Simulation study on a 3-phase SEIG of rating 3.7 kW, 230 V, 1440 rpm operating in standalone mode with excitation capacitor bank of 4 kVAR and DC link voltage of VSC 400 V is carried out under varying nonlinear load.

#### 4.3.1 Generation of Control Signals of VSC using LMA Control Algorithm

The LMA control technique is simulated in MATLAB/Simulink to generate control signals of the VSC for regulating three phase terminal voltages of SEIG, ( $v_{sabc}$ ) and frequency (F). The magnitude of SEIG terminal voltage ( $v_t$ ) is determined from the sensed value of three phase voltages ( $v_{sa}, v_{sb}, v_{sc}$ ). The active components ( $u_{pa}, u_{pb}, u_{pc}$ ) of unit templates are generated by dividing three phase instantaneous voltages ( $v_{sa}, v_{sb}, v_{sc}$ ) by magnitude of the terminal voltage ( $v_t$ ). Further, reactive component of unit templates ( $u_{qa}, u_{qb}, u_{qc}$ ) are derived from active components of unit templates ( $u_{pa}, u_{pb}, u_{pc}$ ) by using delay elements.

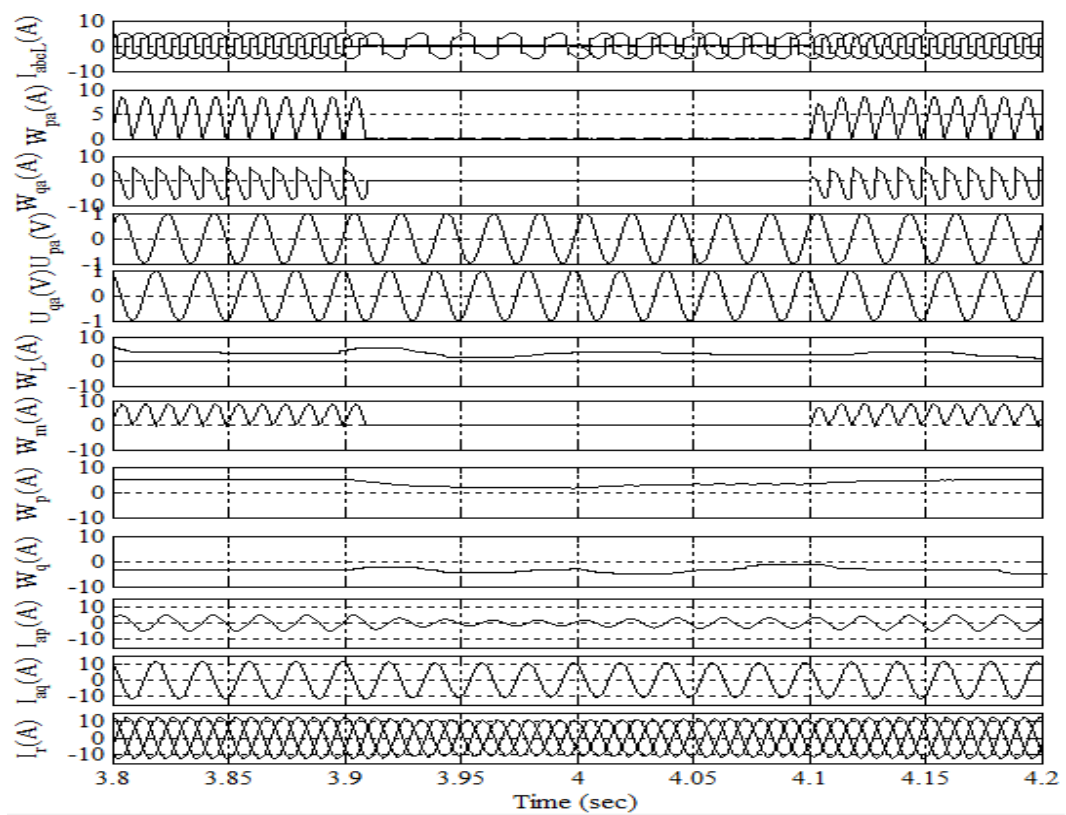


Fig. 4.3 Simulation Results of Reference Current Generation Process

The waveforms of phase 'a' unit templates' reactive component ( $u_{qa}$ ) and active component ( $u_{pa}$ ) of source current have been shown in Fig.4.3, which are in quadrature with each other. The LMA control is being used to update the fundamental active and reactive component ( $u_{pa}, u_{pb}, u_{pc}$ ) and ( $u_{qa}, u_{qb}, u_{qc}$ ) of the load current ( $i_{abcl}$ ) are presented in Fig.4.3. The LMA updates these active and reactive components of three-phase templates ( $w_{pa}, w_{pb}, w_{pc}$ ) and ( $w_{qa}, w_{qb}, w_{qc}$ ) respectively till the error in unit templates and load currents are converged. After

determining the error between load current and unit templates of active and reactive currents separately, the leaky and momentum term of the weights i.e.,  $W_L$  and  $W_m$  are calculated and active and reactive components of error templates are updated accordingly. Under varying load conditions, the variation of these weights ( $W_L$ ,  $W_m$ ) is shown in Fig.4.3. It is observed that leaky weight factor ( $W_L$ ) is varied as the load current ( $i_{abcL}$ ) changes. The average active weight of all three phase ( $W_p$ ) and average reactive component weight factor ( $W_q$ ) are determined to obtain the magnitude of active power component of load current. The variation of these weights is also shown in Fig.4.3. Total magnitude of reference active real power component of load current is calculated through sum of average active weight ( $W_L$ ) and frequency, proportional integral output. The summation block output is multiplied with active unit templates of the reference load current and generated reference current corresponding to fundamental load current component ( $I_{Lp}$ ). Similarly, the output of PI controller is deducted from the average weight of reactive currents for regulating the terminal voltage to determine magnitude for component of reactive power of the load ( $I_{aq}$ ). These active and reactive reference currents are shown in Fig.4.3.

### **4.3.2 LMA Control Algorithm Performance for Voltage and Frequency Control under Load Variation on SEIG System**

Fig.4.4 shows the variation of the SEIG terminal voltages ( $v_{abc}$ ), currents ( $i_{abcS}$ ), nonlinear load currents ( $i_{abcL}$ ), VSC currents ( $i_{abcC}$ ), frequency (F) and dc-link voltage V, while worst case switching in load from 3-phase to 1-phase and subsequently 2-phase conditions. It is observed that SEIG is started with initial 3-phase load with terminal phase voltages about 130V (rms). At  $t=3.9$  sec. the load currents in phase 'b' and 'c' are suddenly interrupted causing severe unbalance in load current i.e.,  $i_b = i_c = 0$ ,  $i_a = i_{aL}$ . However, due to

the presence of VSC, the SEIG terminal currents are still balance, and as VSC supplement the necessary load current and therefore the compensating currents ( $i_{abcC}$ ) of VSC are also unbalanced till unbalance in the load sustain till  $t = 4.1$  sec. Further, it is clear that the SEIG phase voltage ( $v_{abc}$ ) remain balanced despite the unbalances in the load. Also, the frequency (F) of the system remains in close proximity of 50 Hz, since the battery energy storage system at DC link ensure balance between power generated and power consumed during variations of load. The theoretical values of voltage and frequency in steady state is shown in Table 4.1.

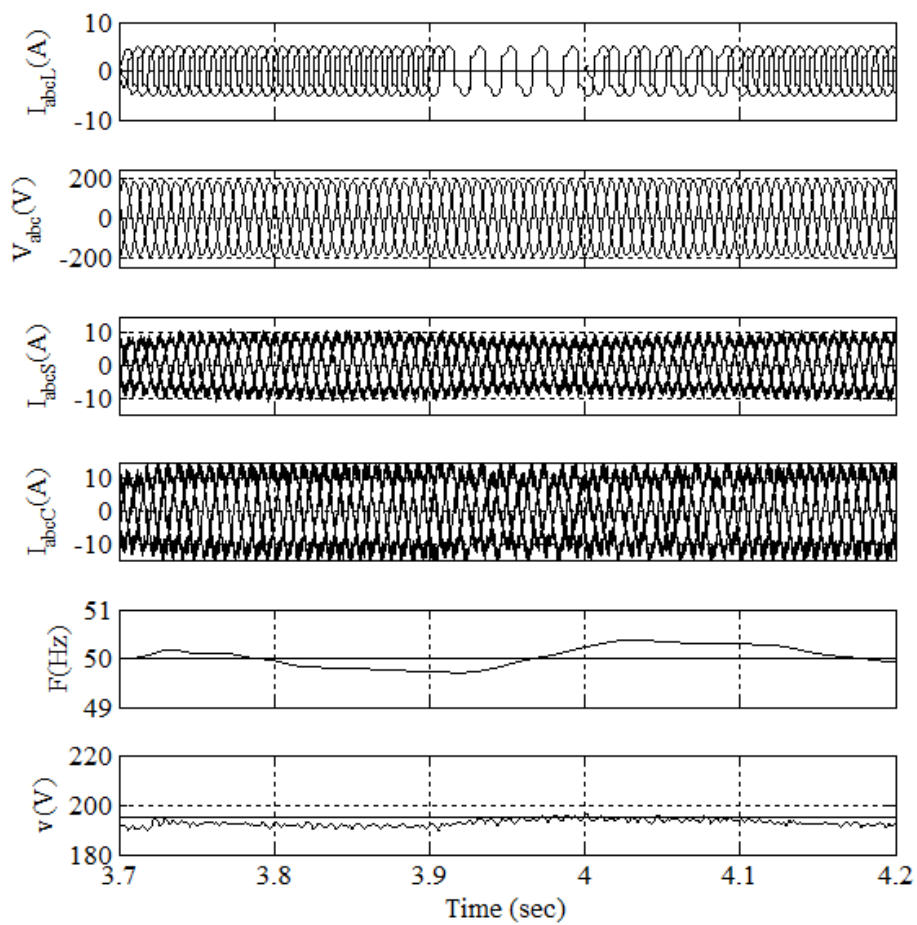


Fig. 4.4 Simulation results using LMA Control Algorithm for voltage and Frequency Control of SEIG under Load Variation

Table 4.1 Voltage and Frequency Control Operation

Sr. No.	Electrical Parameters	Nominal Value	Steady state error	Settling
1	Phase Voltage (V)	184 V Peak	1-2 V	2 Cycles
2	Frequency (f)	50 Hz	$\pm 0.05$ Hz	3 Cycles

### 4.3.3 Power Balance during sudden change in Load

Fig.4.5 shows the variation of load currents ( $i_{abcL}$ ), SEIG terminal voltage ( $v_{abc}$ ), the generated real power ( $P_g$ ), real power consumed in the load ( $P_L$ ) and real power support from VSC ( $P_c$ ) and power in BESS ( $P_b$ ). It is observed that during  $t = 3.72$  second to  $t = 3.9$  second, when load is constant, SEIG generates 2 kW out of which about 1.5 kW is consumed in fixed nonlinear load and balance 500W is being utilized in charging of BESS at DC link of VSC. When loads of phases 'b', and 'c' are suddenly opened at  $t = 3.9$  sec. and load power is reduced to a about 500 W, the VSC absorb more real power in BESS and the difference between generated power ( $P_g$ ) and power consumed ( $P_L + P_c$ ) are maintained and therefore the frequency (F) of the system is maintained close to 50 Hz even in isolated mode of operation of SEIG. The numerical values of different powers in steady state operation of system are shown in Table 4.2.



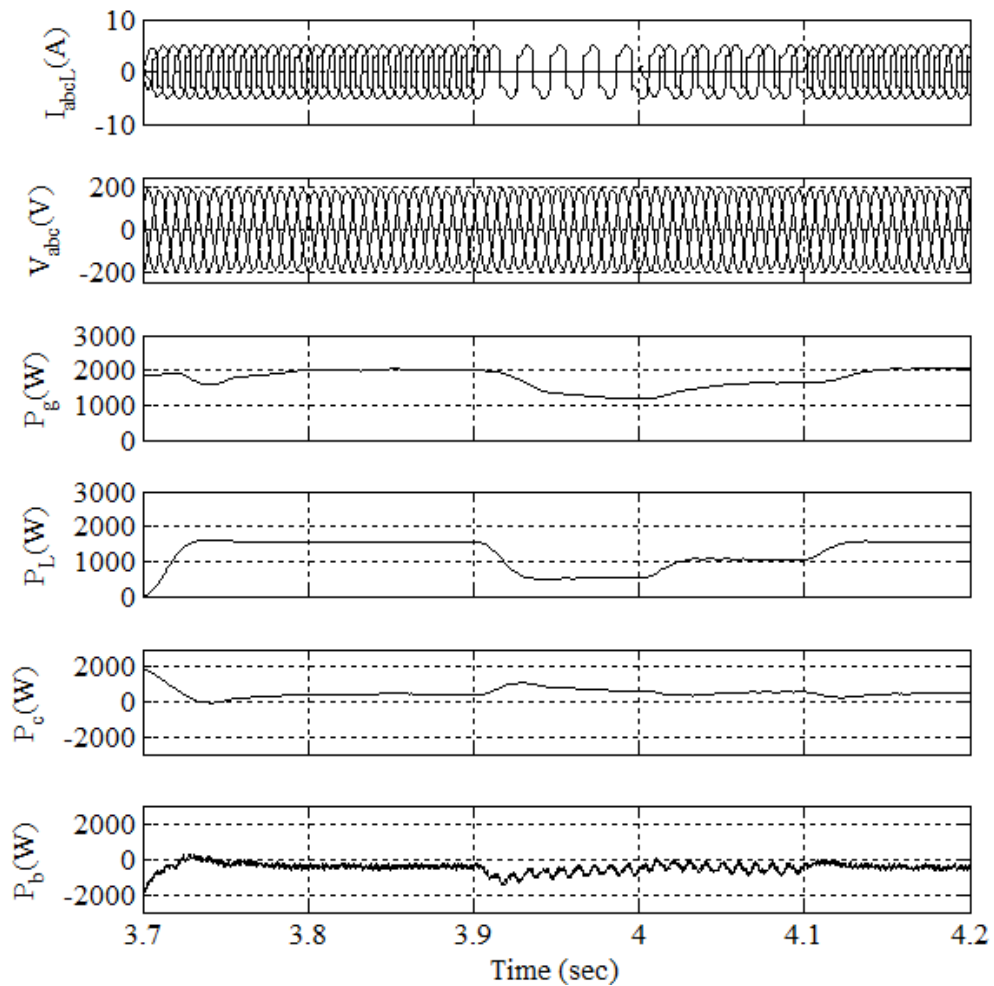


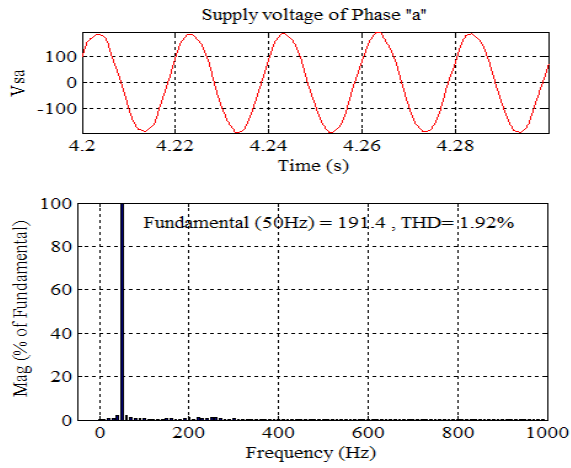
Fig. 4.5 Simulation performance of LMA during power dynamics of system

Table 4.2 Steady State Load Balance Operation

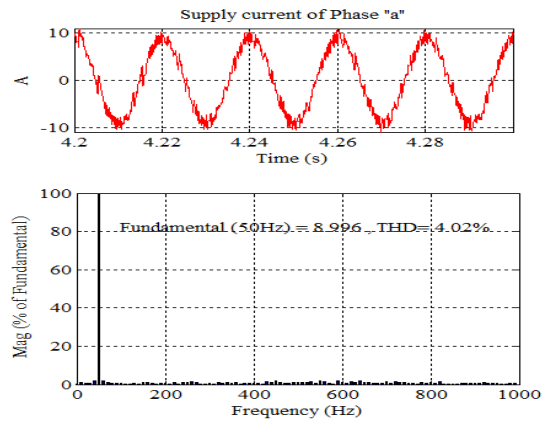
Sr. No.	$P_g$	$P_L$	$P_c$	$P_b$
1.	2000 W	1600 W	400 W	-400 W

#### 4.3.4 Power Quality Indices in Steady State Condition

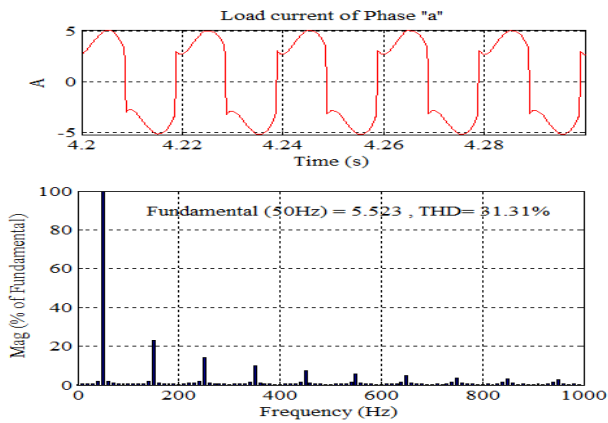
Fig. 4.6(a), 4.6(b) and 4.6(c) shows THD in SEIG terminal voltage ( $v_a$ ), SEIG phase 'a' current ( $i_a$ ) and load current ( $i_L$ ) under steady state conditions. THD observed in terminal voltage is only 1.9 %. Further, the load being nonlinear has very high THD it's about 31.31%, but still the SEIG terminal current THD is about 4.02%. These values of THD are also depicted in Table 4.3. It is clear that LMA is not only effective in regulating voltage and frequency of SEIG based isolated energy generation systems but equally well in elimination of harmonics from source currents.



(a)



(b)



(c)

Fig.4.6 Simulation Results of Harmonic distortion in steady state (a) THD in phase 'a' of supply voltage (b) THD in phase 'a' of supply current (c) THD in Load current of phase 'a'

Table 4.3 Power Quality Indices in Steady State

Sr. No.	THD in $I_s$	THD in $V_s$	THD in $I_L$
1	4.02 %	1.92 %	31.31 %

#### 4.4 Experimental Performance

Fig. 4.7 shows the photograph of the proto-type experimental set-up developed in the laboratory to validate the simulation study. The experimental results on the developed system are recorded using a 4- channel DSO. The system comprises power circuit and control circuit. The generator, 3 leg intelligent power module of VSC based on IGBT switches, dc link capacitor, battery energy storage system, interfacing inductors and nonlinear load comprising of 3-single phase diode rectifier with inductive load on dc side of the rectifier are the part of power circuit. The major component of control circuit is digital controller board d-SPACE 1104. There are 8 ADC channels out of which four are multiplexed and remaining four are available without any multiplexing. Also, there are 8 independent DAC's available with high quality resolution. The voltage handling capacity of ADC is bipolar 10 V. The LEM based LA 55 and LV 25 current and voltage sensors are used for signal conditioning purpose. The seven optocoupler ICs 6N136 are used for optical isolation between controller and IGBT gate driver circuit. The similar number of transistor TL 2N2222 are used to configure this circuit. It required 0-5V DC supply and transistor amplifier amplify to 15 V level. For recording of real time waveforms one four channels KEYSIGHT DSO-X 2004A is used for capturing the dynamics waveforms of the system. The waveforms are also recorded single phase power quality analyzer of FLUKE make-43B for harmonics analysis of the waveforms. The entire system performance is divided into two parts. The first part belongs to dynamic state and other part belongs to steady state performance of the system which are discussed below.

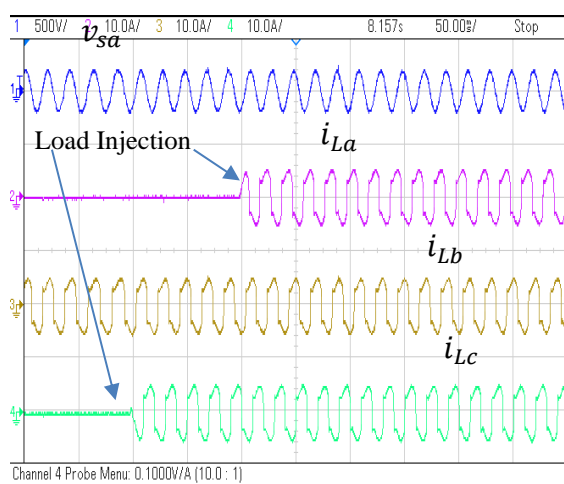


Fig. 4.7 A photograph of the proto-type experimental set-up developed in laboratory

#### 4.4.1 The Experimental results under sudden change in System Dynamics

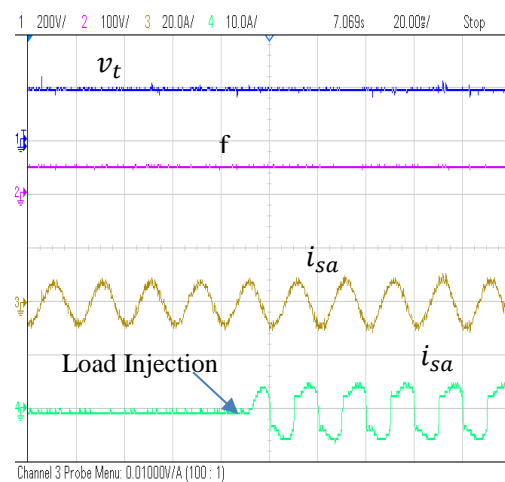
The system dynamics is studied during experimentation and shown in Fig. 4.8 (a-f). The effect of load current variation ( $i_{La}$ ,  $i_{Lb}$ ,  $i_{Lc}$ ) on source voltage ( $v_{sa}$ ) is studied in Fig. 4.8 (a). It is evident from the observation of result that the dynamics in load is created by switching off the load from phase ‘a’ and phase ‘c’. It is also observed that there is no variation in the voltage magnitude as well as frequency of the supply voltage ( $v_{sa}$ ). It means that due to proper control action of the proposed LMA control, voltage and frequency remains unaltered. The Fig. 4.8 (b) depicts the effect of load dynamics ( $i_{La}$ ) and its nonlinearity on supply current ( $i_{sa}$ ), terminal voltage ( $v_t$ ) and frequency ( $f$ ). From this result, it is clear that despite the load current variation in phase ‘a’, the supply current is continuous and sinusoidal. The terminal voltage and frequency are also maintained at constant value. The validity of Kirchhoff’s current law is tested and presented in Fig. 4.8 (c). It is clear from the observed result that the supply current of phase ‘a’ is equal to compensator current of the same phase when load is disconnected from the phase ‘a’. The load balancing performance of the proposed control algorithm is verified experimentally and presented in Fig.4.8 (d). From the results, it is clear that the generator is

always supplying the balance current from its all phases though the load current is unbalanced. The unbalanced is created by switching actions in phase ‘a’ of the load. The neutral current compensation and frequency of the zero-sequence current under unbalanced and balanced condition is verified and presented in Fig. 4.8 (e). When loads are balanced the three time of fundamental frequency is observed and it was expected also. From the dynamic performance of the proposed control, it is concluded that the system performance is satisfactory and as per standards.



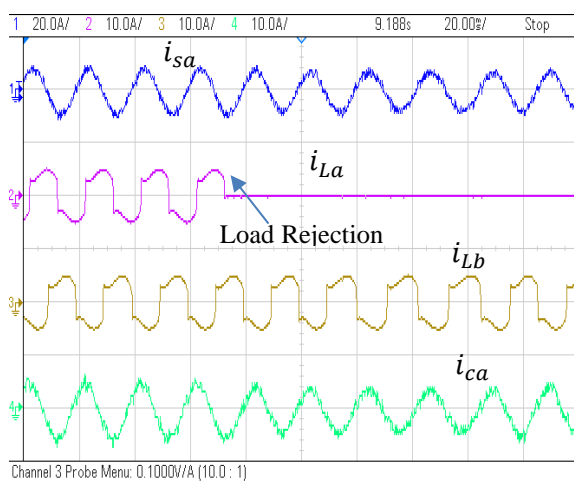
(a) On horizontal axis- time/div (50ms/div)

On vertical axis- Channel 1- Source voltage ( $v_{sa}$ ), channel 2-Load current of phase ‘a’ ( $i_{La}$ ), channel 3-Load current of phase ‘b’ ( $i_{Lb}$ ), channel 4-Load current of phase ‘c’ ( $i_{Lc}$ ).

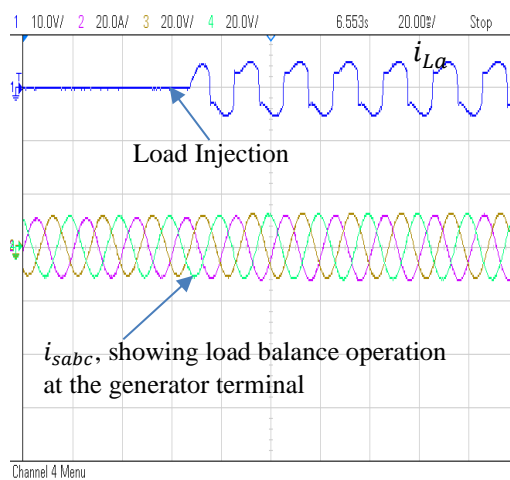


(b) On horizontal axis- time/div (20ms/div)

On vertical axis- Channel1- PCC amplitude voltage ( $v_t$ ), channel 2-frequency ‘f’, channel 3-source current of phase ‘a’ ( $i_{sa}$ ), channel 4-Load current of phase ‘a’ ( $i_{La}$ ).

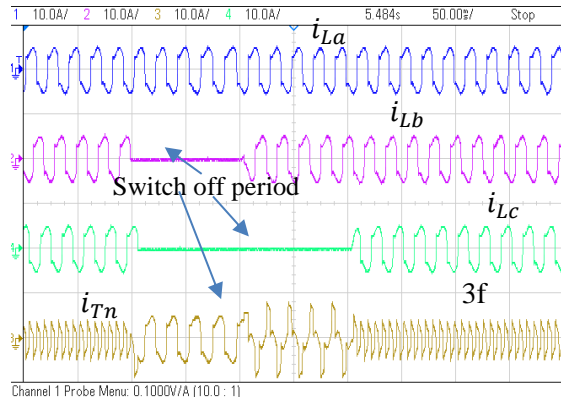


(c) On horizontal axis- time/div (20ms/div)



(d) On horizontal axis- time/div (20ms/div)

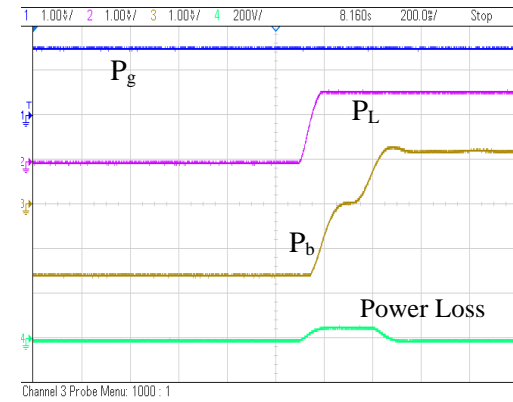
On vertical axis- Channel1- Source current ( $i_{sa}$ ), channel2- Load current of phase 'a' ( $i_{La}$ ), channel3-Load current of phase 'b' ( $i_{Lb}$ ), channel4-compensator current of phase 'a' ( $i_{ca}$ ).



(e) On horizontal axis- time/div (50ms/div)

On vertical axis- Channel1- Load current of phase 'a' ( $i_{La}$ ) channel 2- Load current of phase 'b' ( $i_{Lb}$ ), channel 3- Load current of phase 'c' ( $i_{Lc}$ ), channel 4- Transformer neutral current ( $i_{Tn}$ ).

On vertical axis- Channel1- Load current of phase 'a' ( $i_{La}$ ), channel 2,3,4 source current of phase 'a, b, c' ( $i_{sabc}$ ).



(f) On horizontal axis- time/div (200ms/div)

On vertical axis- Channel1- Generator power ( $P_g$ ) channel 2- Load power ( $P_L$ ), channel 3- Battery power ( $P_b$ ), channel 4- power loss.

Fig.4.8 Experimental performance of proposed control with system under study and waveforms of (a) variations in source voltage ( $v_{sa}$ ) with load current dynamics ( $i_{La}$ ,  $i_{Lb}$ ,  $i_{Lc}$ ), (b) study of  $v_t$ ,  $f$ ,  $i_{sa}$  with  $i_{La}$ , (c)  $i_{sa}$ ,  $i_{La}$ ,  $i_{Lb}$ ,  $i_{ca}$ ), (d) load balancing of  $i_{sabc}$  with  $i_{La}$ , (e) study of zero sequence current  $i_{Tn}$  with load current dynamics ( $i_{La}$ ,  $i_{Lb}$ ,  $i_{Lc}$ ), (f) Steady state performance and powers of generator ( $P_g$ ), Load ( $P_L$ ) and battery ( $P_b$ ) and loss in the system.

#### 4.4.2 The Experimental performance under Steady State Condition of the system

The steady state performance of the system under study is carried out experimentally and presented in Fig. 4.8 (f). The active power sharing between generator, load and battery energy storage unit is discussed here for readers understanding. It is clear from the results that when no load is applied, all the real power generated ( $P_g$ ) is equal to ( $P_b$ ). It means power generated under no load conditions is stored in battery system. However, when load ( $P_L$ ) is applied over the generator terminal, the charging of the battery or in other words storage power of the battery weakens. Moreover, when load power is exceeding the upper limit of generator power, battery started discharging means its power became opposite polarity of its own previous one. From

this observation, it is concluded that the real power match is always maintained by the proposed control algorithm with good accuracy, effectiveness and speed.

#### **4.5 Conclusions:**

The findings of this chapter are summarized as below

1. The Leaky momentum control algorithm is mathematically modelled on the basis of research problems.
2. The entire setup including Control Algorithm is modelled in MATLAB/Simulink.
3. The simulation study of said control is carried out under load dynamics and simulation results found as per expectation. The control algorithm has responded within one cycle to track the load variation under transient conditions.
4. The experimental validation of the control algorithm is also carried out and results are found satisfactory.

# CHAPTER 5

## IMPLEMENTATION OF MODIFIED NLMS CONTROL ALGORITHM FOR COORDINATED OPERATION IN THREE-PHASE WIND-ENERGY CONVERSION SYSTEM

---

### 5.1 General

In this chapter, a modified NLMS (new least mean square) control technique is designed and implemented to estimate the parameters of distributed generation system. Wind energy systems are deployed in remote areas specially where grid supply is either not available or difficult to maintain due to rough weather conditions. In such standalone power system voltage and frequency are vulnerable to change with varying loads or variation in wind conditions. The VSC with advance control can mitigate most of the power quality issues in such system like reactive power compensation, load balancing, power balancing and harmonics eliminations etc. These standalone systems may consist of BES system for providing back up during bad weather conditions and means of storage during light load conditions and can provides capability to such system in managing intermittency of wind energy. This control algorithm enables VSC to regulate the frequency and voltage of the SEIG based wind energy conversion system. A schematic diagram of wind energy based distributed generation system using modified NLMS control algorithm for VSC is shown in Fig. 5.1

### 5.2 Modified NLMS algorithm: An Introduction

The conventional LMS algorithm is one of the most popular adaptive algorithms which has been widely used in estimation and control but it suffers from problem of drifting, wherein the algorithm generates unbounded parameter estimates for a bounded input sequences result in divergence of weight update equations. It is known that a large step size may lead to fast convergence but big mis-adjustment and small step size may provide small mis-adjustment but slow convergence. The modified NLMS algorithm is a class of adaptive control technique,



which has better convergence than LMS but it involves computational complexity. The modified NLMS resolves the problem of drifting by bounding parameter estimates and modified part improves the convergence rate.

The main aim of using modified NLMS algorithm is to estimate accurately fundamental active and reactive components of nonlinear load current during steady state and dynamic load conditions. The weight update equation of the standard LMS algorithm is given by [40].

$$w(n) = w(n-1) + \alpha(n)x(n). \quad (5.1)$$

It can be seen from (5.1) that the filter coefficients are updated by the addition of previous stage weight vector ( $w(n-1)$ ) and a weighted input signal  $x(n)$ . Therefore, the aim of the adaptive filtering is to find a proper weight  $\alpha(n)$  for faster convergence as well as true estimation of filter coefficients. In order to achieve the same, the conventional NLMS algorithm employs the squared posteriori error as its cost function [92],[93],[94] which is given by

$$\varepsilon^2(n) = d^2(n) - 2d(n)w^T(n)x(n) + w^T(n)x(n)x^T(n)w(n) \quad (5.2)$$

Where  $d(n)$  is the distortion or independent surplus noise.

Meanwhile, the weight  $\alpha(n)$  can be found by minimizing (5.2). After some straightforward mathematical manipulations, one has

$$\alpha(n) = e(n)[x^T(n)x(n)]^{-1}. \quad (5.3)$$

To trade off the convergence speed and the misadjustment as well as avoid dividing by zero, a step size  $\mu$  and regularization parameter  $\delta$  are introduced as follows:

$$\alpha(n) = 2\mu e(n)[x^T(n)x(n) + \delta]^{-1}. \quad (5.4)$$

The step size  $\mu$  and a regularization factor  $\delta$  makes NLMS algorithm very difficult in practice, so an updated cost function, with a variable regularization factor  $\beta$  ( $\beta > 0$ ), is used as follows:

$$\xi(n) = \varepsilon^2(n) + \beta [w(n) - w(n-1)] \quad (5.5)$$

To minimize (5.5), one can substitute (5.1) into it and calculate the derivative of  $\xi(n)$  on  $\alpha(n)$  as follows:

$$\begin{aligned}\partial \xi(n) / \partial \alpha(n) &= \{2 \varepsilon(n) \partial \varepsilon(n) / \partial \alpha(n)\} + 2 \beta \alpha(n) \mathbf{x}^T(n) \mathbf{x}(n) \\ &= 2[d(n) - \mathbf{w}^T(n-1) \mathbf{x}(n) - \alpha(n) \mathbf{x}^T(n) \mathbf{x}(n)] \times [-\mathbf{x}^T(n) \mathbf{x}(n)] + 2 \beta \alpha(n) \mathbf{x}^T(n) \mathbf{x}(n).\end{aligned}\quad (5.6)$$

Let  $\partial \xi(n) / \partial \alpha(n) = 0$ , the weight  $\alpha(n)$  can be obtained as

$$\alpha(n) = \{d(n) - \mathbf{w}^T(n-1) \mathbf{x}(n)\} / (\mathbf{x}^T(n) \mathbf{x}(n) + \beta) \quad (5.7)$$

Substituting (5.7) into (5.1), we have

$$\begin{aligned}\mathbf{w}(n) &= \mathbf{w}(n-1) + [d(n) - \mathbf{w}^T(n-1) \mathbf{x}(n)] \mathbf{x}(n) / [\mathbf{x}^T(n) \mathbf{x}(n) + \beta] \\ &= \mathbf{w}(n-1) + [e(n) \mathbf{x}(n)] / [\mathbf{x}^T(n) \mathbf{x}(n) + \beta]\end{aligned}\quad (5.8)$$

which constitutes our modified NLMS adaptive filtering algorithm with a variable regularization factor  $\beta$  ( $\beta > 0$ ) [40]. The implementation of the modified NLMS Control algorithm for power quality assessment of distributed power generation system comprising the three-phase induction generator is given here in the subsequent section.

### **5.2.1 Evaluation of peak value of SEIG terminal voltage, in-phase and quadrature unit vectors**

The peak value ( $V_m$ ) of the terminal voltage of wind driven SEIG is evaluated as

$$V_m = \left( \sqrt{2(v_{sa}^2 + v_{sb}^2 + v_{sc}^2)} / 3 \right) \quad (5.9)$$

$v_{sa}$ ,  $v_{sb}$  and  $v_{sc}$  are the instantaneous phase voltages at point of common interfacing (PCI).

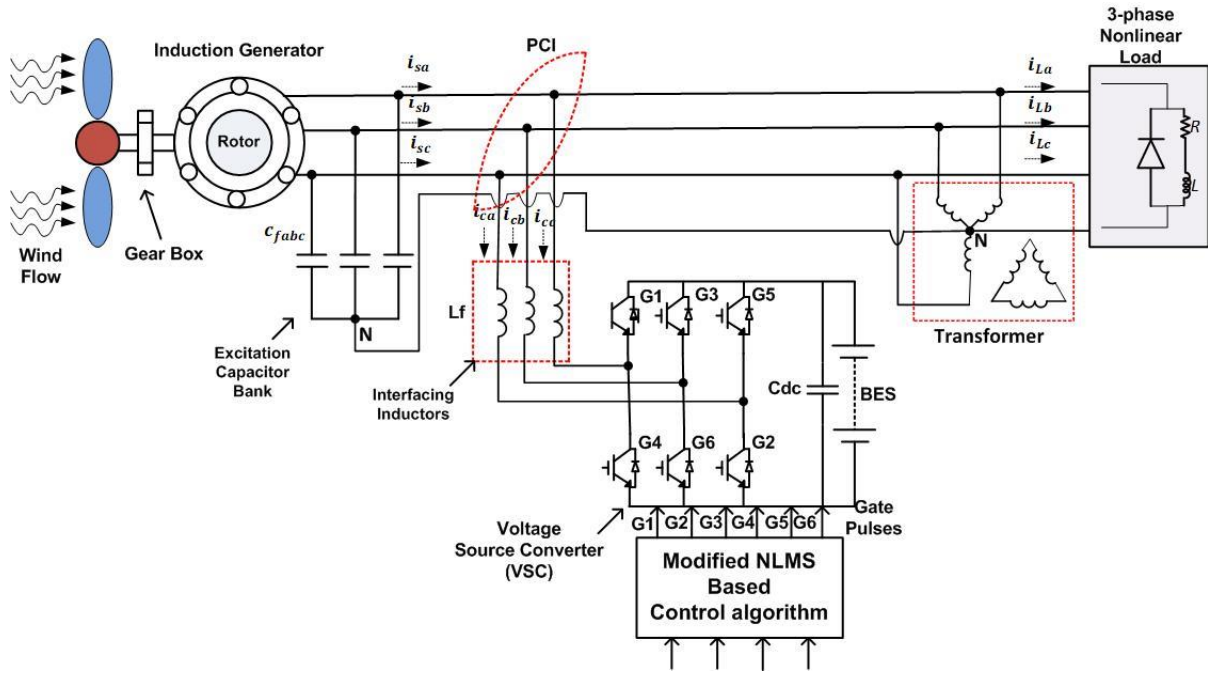


Fig. 5.1 Schematic diagram of distributed generation (DG) system based on Modified NLMS Control Algorithm

The in-phase and quadrature unit vectors are determined as

$$p_{ua} = \frac{v_{sa}}{V_m}, p_{ub} = \frac{v_{sb}}{V_m}, p_{uc} = \frac{v_{sc}}{V_m} \quad (5.10)$$

$$\begin{bmatrix} q_{ua} \\ q_{ub} \\ q_{uc} \end{bmatrix} = \frac{1}{\sqrt{3}} \begin{bmatrix} -1 & 0 & 1 \\ \sqrt{3} & 1 & -1 \\ \frac{-\sqrt{3}}{2} & \frac{1}{2} & \frac{-1}{2} \end{bmatrix} \begin{bmatrix} p_{ua} \\ p_{ub} \\ p_{uc} \end{bmatrix} \quad (5.11)$$

Where,  $p_{ua}$ ,  $p_{ub}$  and  $p_{uc}$  are the in-phase unit vector and  $q_{ua}$ ,  $q_{ub}$  and  $q_{uc}$  are the quadrature phase vectors of the 3-phase voltages of the system.

### 5.2.2 Generation of reference source current for VSC

A new modified NLMS control algorithm is implemented for the generation of VSC switching pulses; this modified control depends on the equation (5.12).

$$w(n) = w(n - 1) + \frac{1}{p_{uabc}^T(n)U(n) + \beta} e_{rr}(n)p_{uabc}(n) \quad (5.12)$$

In this modified algorithm, the value of variable regularization factor ( $\beta$ ) is valid for  $\beta > 0$ . [21]. The modified NLMS control technique is applied to modify the fundamental in-phase ( $p_{ua}, p_{ub}$  and  $p_{uc}$ ) and quadrature ( $q_{ua}, q_{ub}$  and  $q_{uc}$ ) unit vectors of the load current. The NLMS based control modifies the in-phase and quadrature weight components of 3-phase templates ( $w_{pa}, w_{pb}$  and  $w_{pc}$ ) and ( $w_{qa}, w_{qb}$  and  $w_{qc}$ ). Frequency error is estimated from the source voltage frequencies and the reference frequency (50Hz), and is fed to the PI regulator for frequency control. The output of frequency PI regulator is added to weight for the in-phase component of load current. The summation of PI regulator current and fundamental active average components of the nonlinear load current generates the active component of reference source current. Similarly, to regulate the AC terminal voltage magnitude, difference of fixed reference voltage and evaluated peak voltage is given to the AC terminal voltage PI controller.

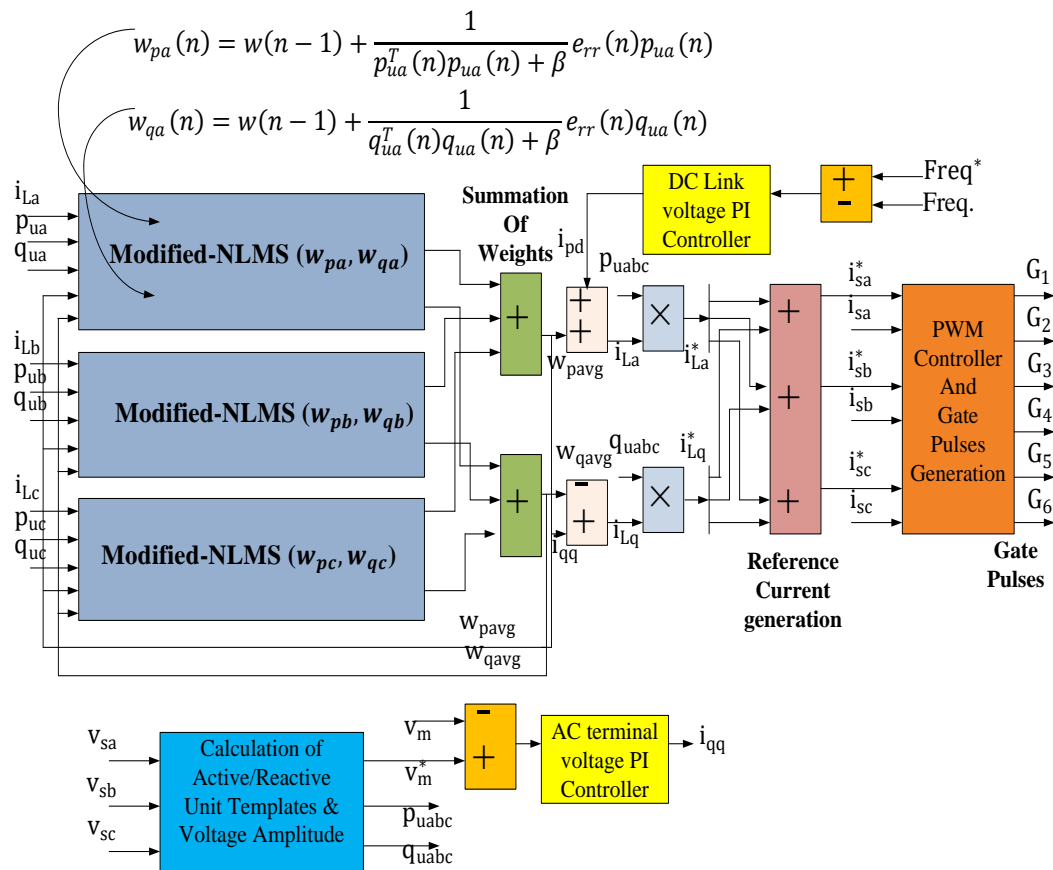


Fig. 5.2 Block diagram of Modified NLMS Control Algorithm

The output of PI controller for terminal voltage regulation is added to the weight for quadrature component of reference source current. The fundamental reactive weight component and PI controller current are used to generate quadrature reference current.

$$i_{La}^* = i_{La} \times p_{uabc} \quad (5.13)$$

$$i_{Lq}^* = i_{Lq} \times q_{uabc} \quad (5.14)$$

The summation of eq. (5.13) and (5.14) give extracted reference source current and the extracted current is purely sinusoidal under nonlinear load condition. The extracted current and reference current of source is fed to the PWM block for the generation of switching pluses of VSC.

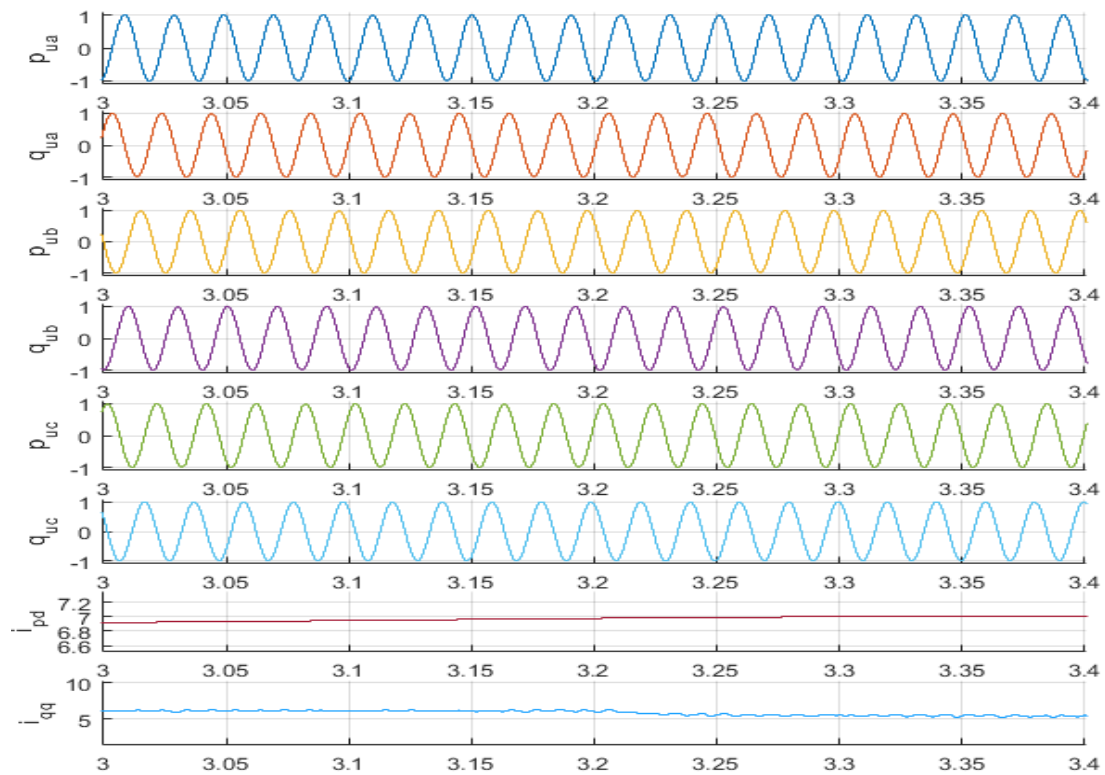
$$i_{sabc}^* = i_{La}^* + i_{Lq}^* \quad (5.15)$$

Control structure of NLMS algorithm for PWM switching of VSC in an isolated wind energy system has been shown in Fig.5.2

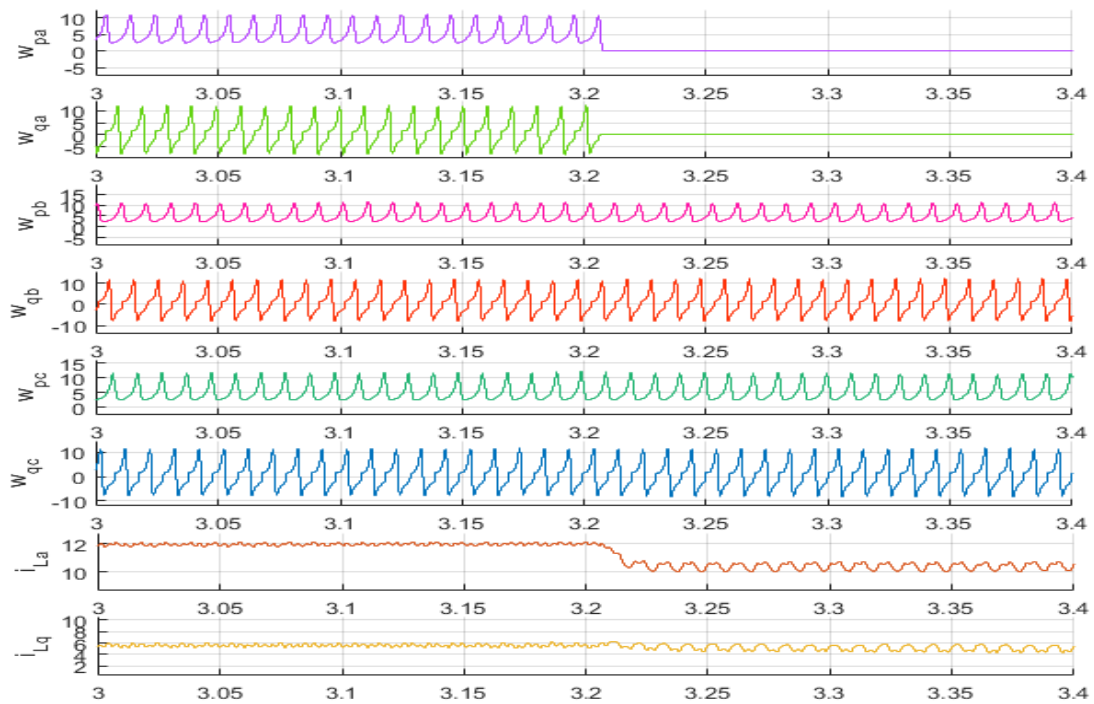
### 5.3 Simulation Study of Modified NLMS Control Algorithm

Simulation study on distributed wind energy conversion system consisting of a 3.7 kW, 230 V, 50 Hz SEIG excited with a capacitor bank of 4 kVAR and supported with a 400 V, 7.5 AH, BESS is carried out in MATLAB/Simulink to demonstrate the application of algorithm to mitigate the power quality issues of this standalone system. Configuration of control scheme for VSC control is shown in Fig. 5.2. Extensive simulation study has been done and its simulation results are shown and analyzed in this section. For the feasibility study of the control algorithm, the designed MATLAB model is simulated under various operating conditions. The control algorithm has been implemented to obtain the multi-objectives power quality improvement in SEIG-based distributed system. The estimation of updated weights of active and reactive load current components, for calculating the reference source current, are obtained

using Modified NLMS control algorithm. Fig. 5.3 to Fig. 5.8 shows the simulation results and detailed descriptions of these results are given in sub-sections 5.3.1 to 5.3.6 as follows:



(a)



(b)

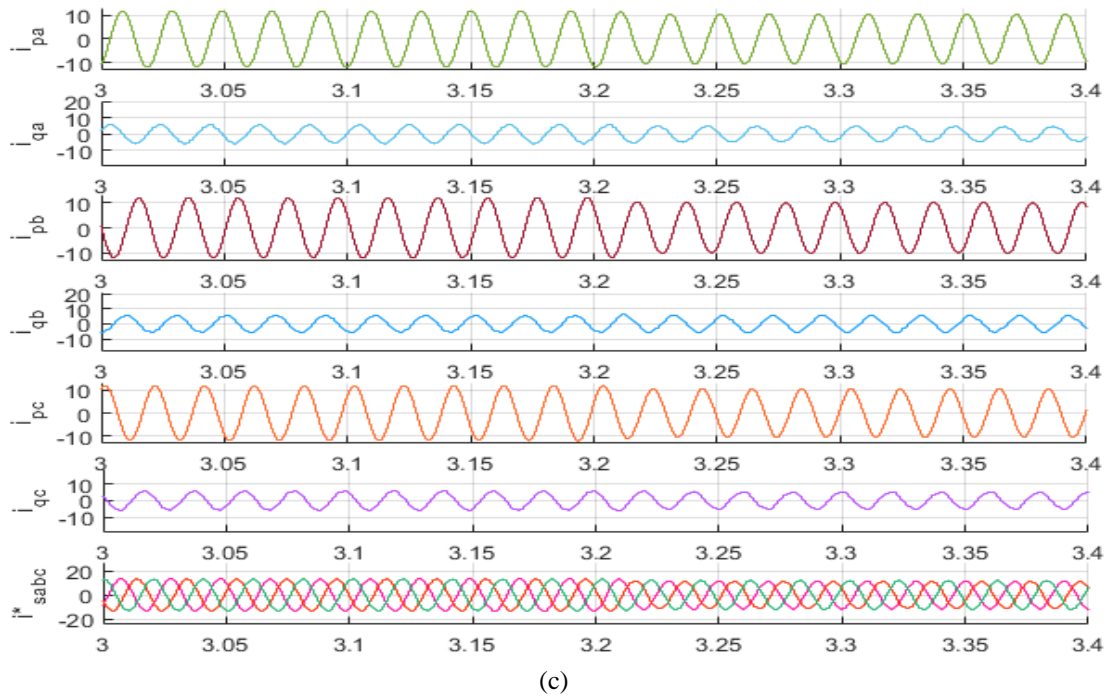


Fig. 5.3 Intermediate signals of modified NLMS algorithm (a) active/reactive unit templates, AC terminal voltage PI controller current and DC link voltage PI controller current (b) Extracted active/reactive weight templates, active/reactive reference current (c) active/reactive current component and extracted reference current

### 5.3.1 Intermediate Control Signal profiles in NLMS Control Algorithm

Fig 5.3 (a), (b) and (c) show the intermediate signals profiles in implementation of modified NLMS based control algorithm for distributed generation system. Fig. 5.3 (a) shows the estimated signals namely  $p_{ua}$ ,  $q_{ua}$ ,  $p_{ub}$ ,  $q_{ub}$ ,  $p_{uc}$ ,  $q_{uc}$ ,  $i_{pd}$  and  $i_{qq}$  under disconnection of load of phase 'a' at  $t=3.2$  sec. The Fig. 5.3(a) control signals show the active/reactive unit templates, DC and AC voltage regulating PI controller current profiles  $i_{pd}$  and  $i_{qq}$ . Fig. 5.3(b) depicts weight updation of the inner control signal  $w_{pa}$ ,  $w_{qa}$ ,  $w_{pb}$ ,  $w_{qb}$ ,  $w_{pc}$ ,  $w_{qc}$ ,  $i_{La}$  and  $i_{Lq}$  under removal of load of phase 'a' at  $t=3.2$  sec. The Fig. 5.3 (b) shows control signals waveforms of the extracted active/reactive components and extracted reference current. Fig. 5.3 (c) shows control signal  $i_{pa}^*$ ,  $i_{qa}^*$ ,  $i_{pb}^*$ ,  $i_{qb}^*$ ,  $i_{pc}^*$ ,  $i_{qc}^*$  and  $i_{sabc}^*$  under disconnection of load of only one phase at  $t=3.2$  sec. The extracted reference source current is purely sinusoidal under nonlinear load condition on the distributed generation system.

### 5.3.2 Steady State Performance of Distributed Generation System Under Fixed Wind Velocity Feeding Fixed Nonlinear Load

Fig. 5.4 shows the steady state performance of distributed generation system under fixed wind velocity (21 m/s) feeding fixed nonlinear load. The NLMS based control stabilizes the system frequency and voltage of distributed generation system while feeding nonlinear loads. The excess power generated other than the nonlinear load is supplied to the battery energy storage (BES) and controller also maintains the DC link voltage.

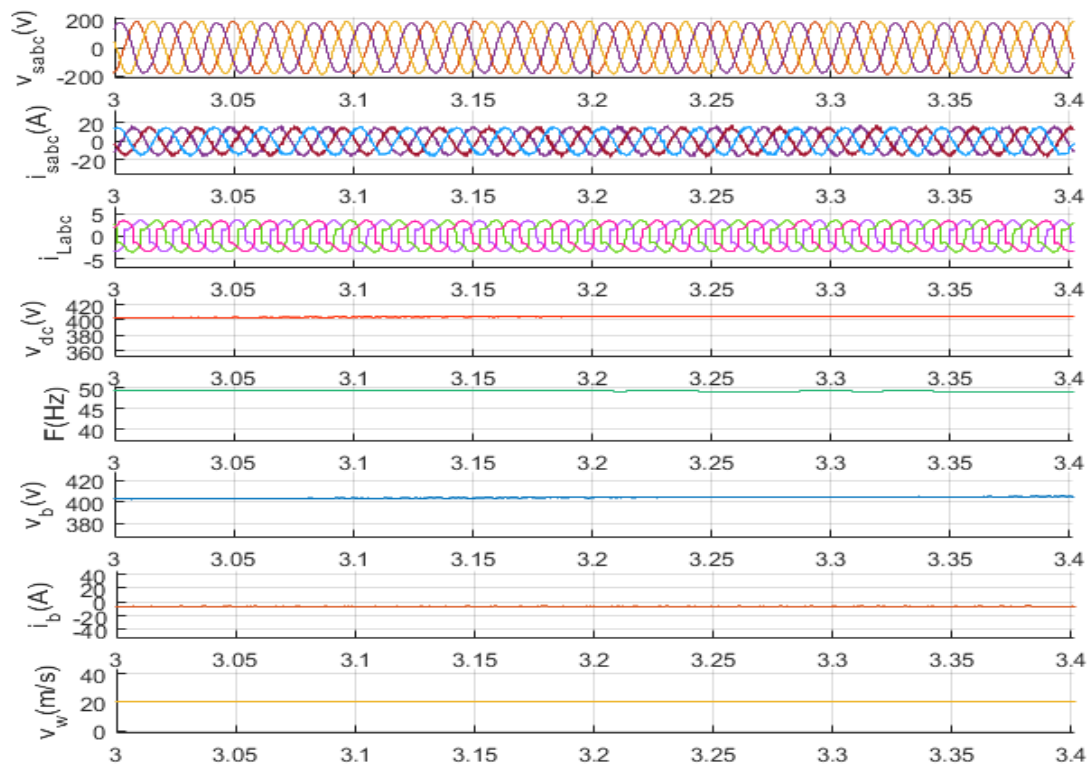


Fig. 5.4 Steady state performance of distributed generation system under fixed wind velocity and fixed load

### 5.3.3 Dynamic Performance of Distributed Generation System Under Varying Wind Velocity Feeding Fixed Nonlinear Load

Fig. 5.5 depicts the dynamic performance of distributed generation system under varying wind velocity feeding fixed nonlinear load. The wind velocity is declined from 21 m/s to 15 m/s at  $t=3.2$  sec. Due to variation in wind speed, the battery current is slightly reduced



and supplying the active power through VSC at PCI, the BES is used to maintain the power balance between the DG system and the load. The modified NLMS based controller maintains the source terminal voltage and sinusoidal source current, DC link voltage and frequency are also maintained constant during reduction in wind velocity.

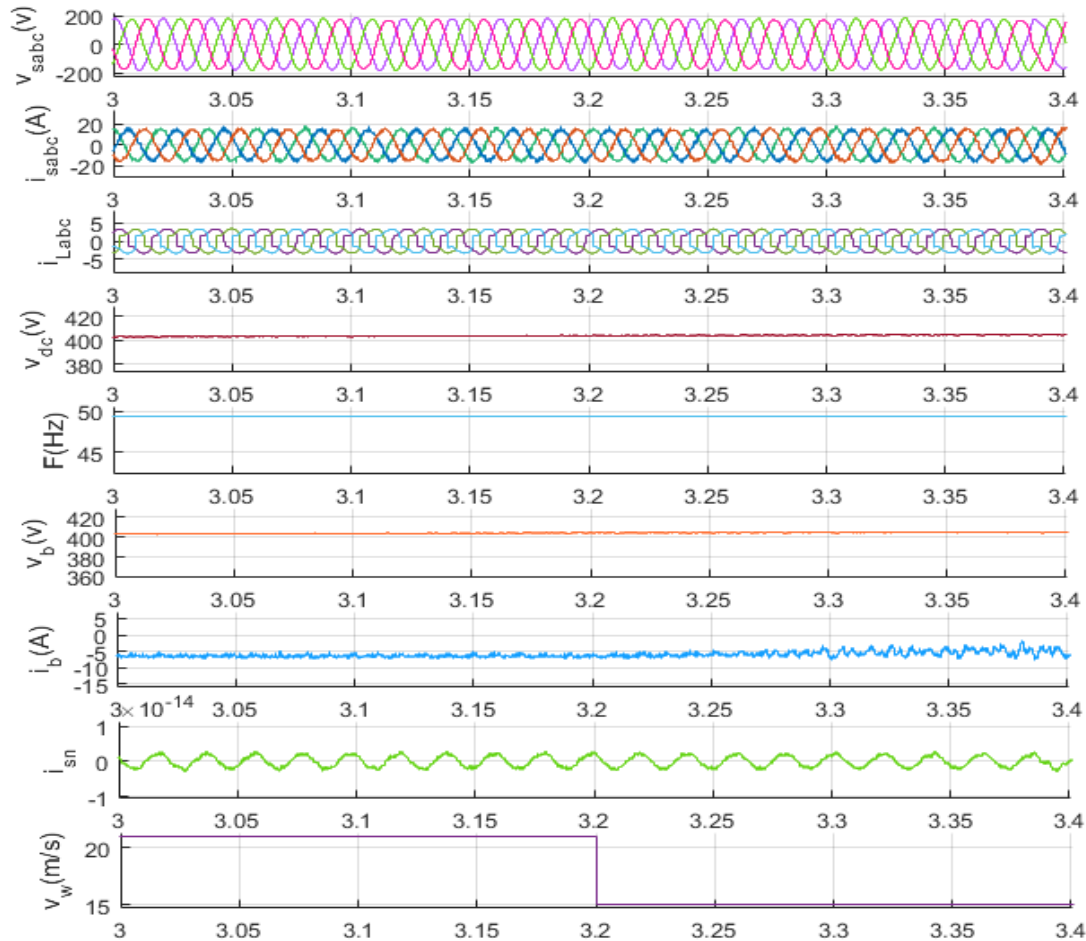


Fig. 5.5 Dynamic performance of distributed generation system under varying wind velocity and fixed load

### 5.3.4 Dynamic Performance of Distributed Generation System Under Fixed Wind Velocity Feeding Varying Nonlinear Load

Fig. 5.6 shows the dynamic performance of distributed generation system under fixed wind velocity feeding varying nonlinear load. The single-phase load of phase ‘a’ is disconnected at  $t=3.1$  sec to  $t=3.3$  sec. During disconnection of load, the load current is

decreased and battery charging current is increased in the period  $t=3.1$  sec. to  $t=3.3$  sec. The simulation results show that controller maintains the source voltage, source current, battery voltage, DC link voltage and neutral current during variation in load. During removal of load, the extra current is supplied to battery storage system (BES), which is interfaced at DC link of VSC.

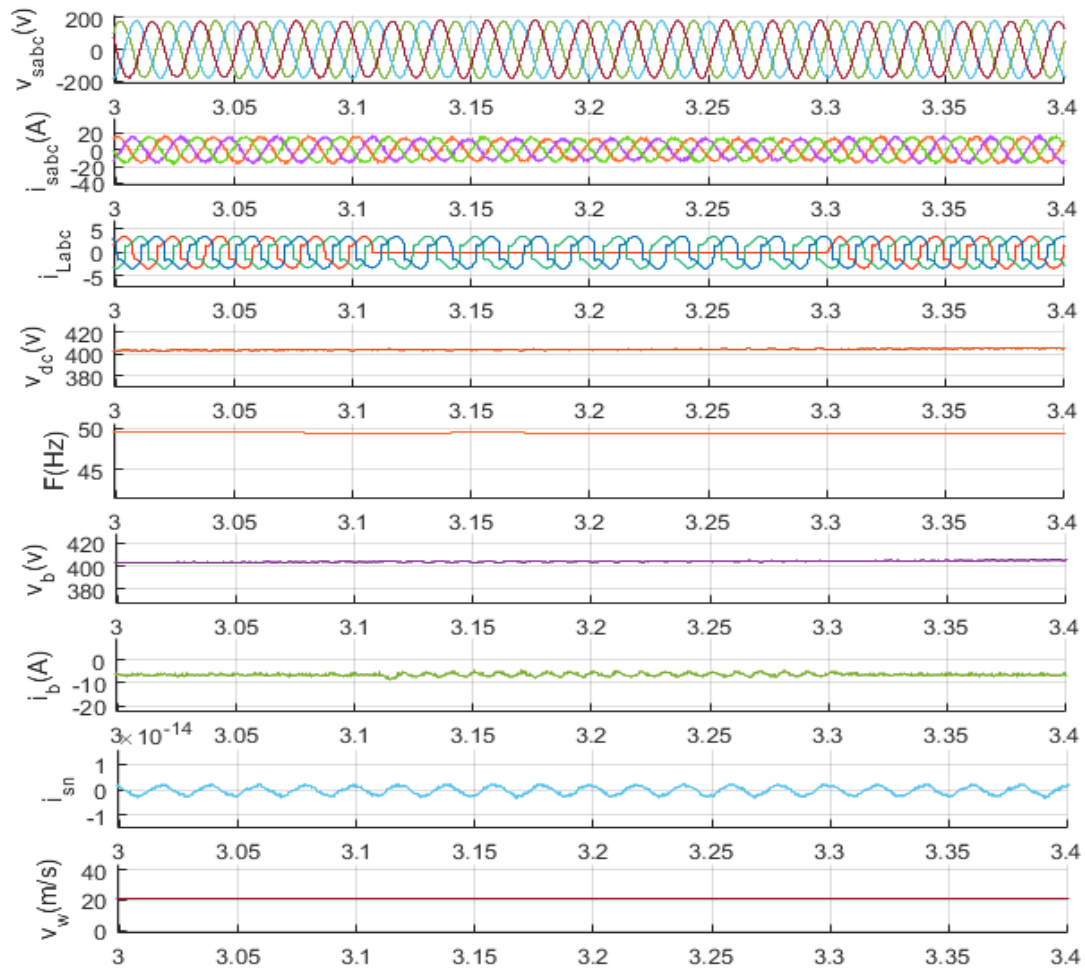
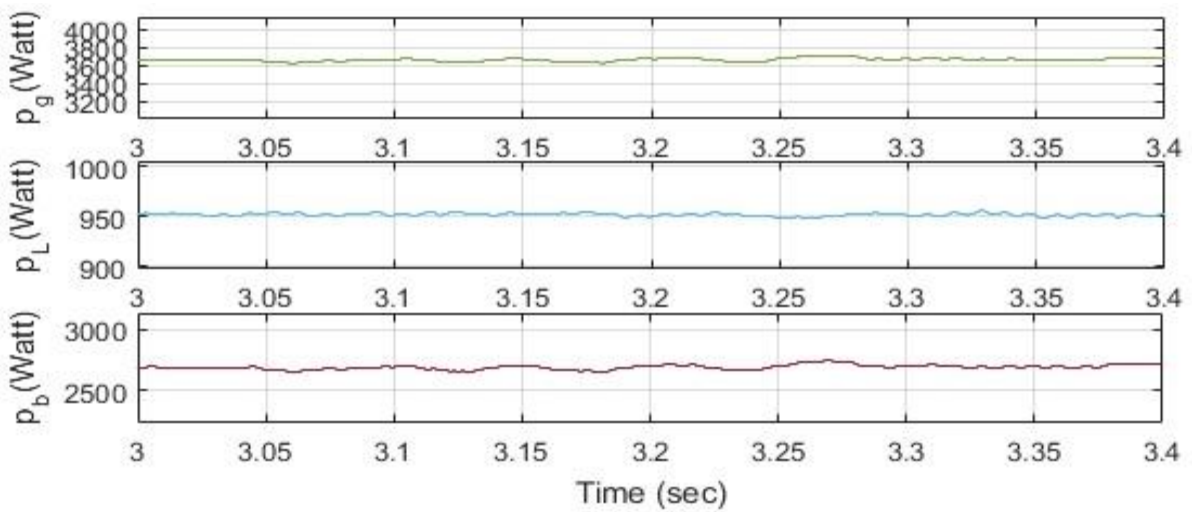


Fig. 5.6 Dynamic performance of distributed generation system under fixed wind velocity and varying load

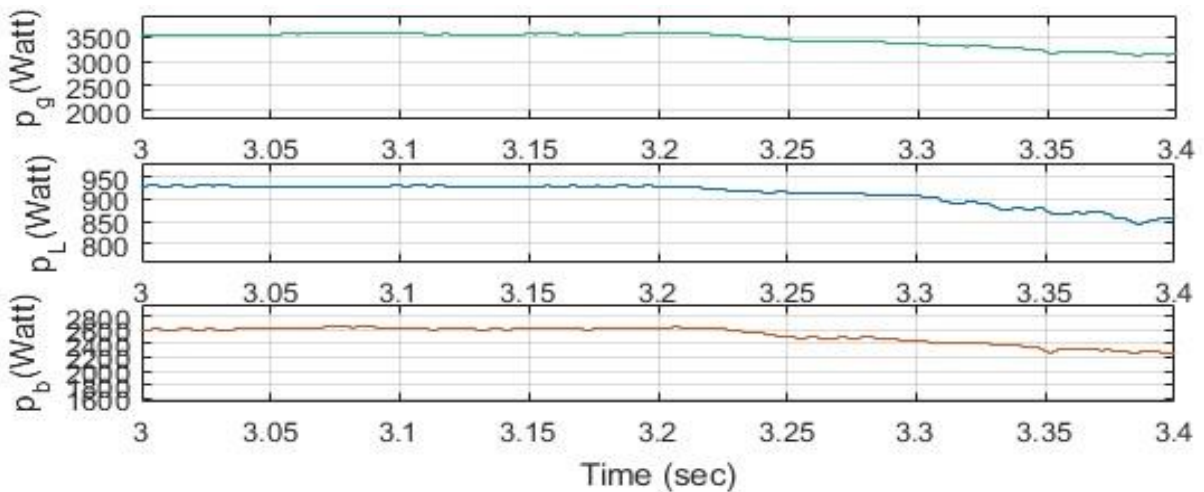
### 5.3.5 Power Quality Indices in Steady State Condition/Power Balance Performance in Load Dynamical Conditions

Fig. 5.7 (a)-(c) shows the power balances of distributed generation system under fixed wind speed feeding nonlinear load. Fig. 5.7 (a) shows the power balance of distributed generation (DG) system under fixed wind velocity and constant load. Fig. 5.7 (b) shows the

power analysis of DG system under varying wind speed and constant load. The wind velocity is reduced at  $t=3.2$  sec, due to reduction in wind speed the generator power, load power and battery power is reduced. Fig. 5.7 (c) shows the power analysis of DG system under fixed wind speed feeding varying nonlinear load. The load is disconnected at  $t=3.1$  sec to  $t=3.3$  sec, during this duration, the generator power and battery power is increased and load power is decreased. The numerical values of powers are provided in Table 5.1.



(a)



(b)

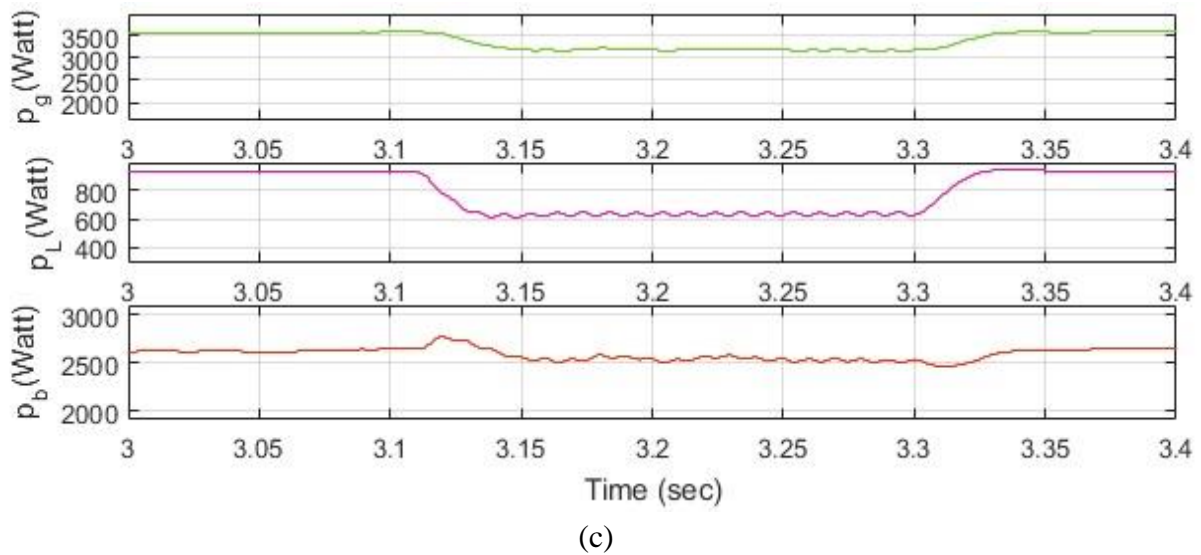


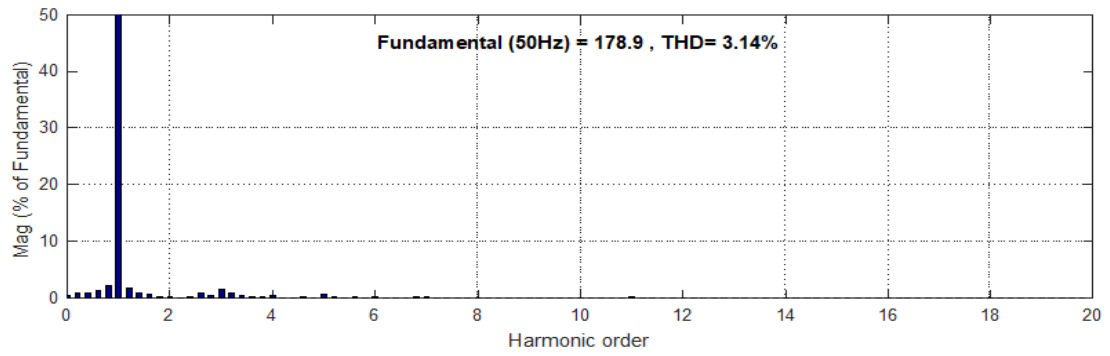
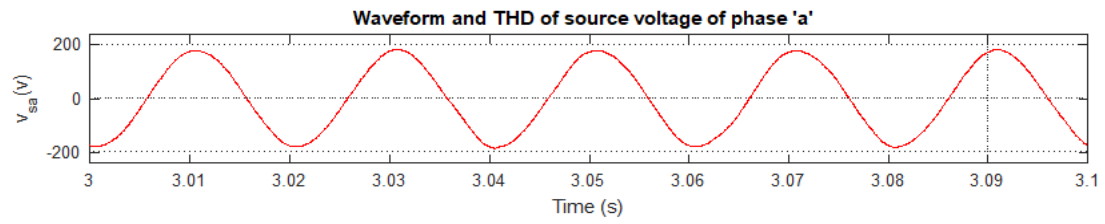
Fig. 5.7 (a)-(c) Power quality indices of DG system a) Generated power b) Load power and c) Battery power under fixed/varying wind velocity feeding fixed/varying nonlinear load

Table 5.1 Power Balance in Different Operating Conditions

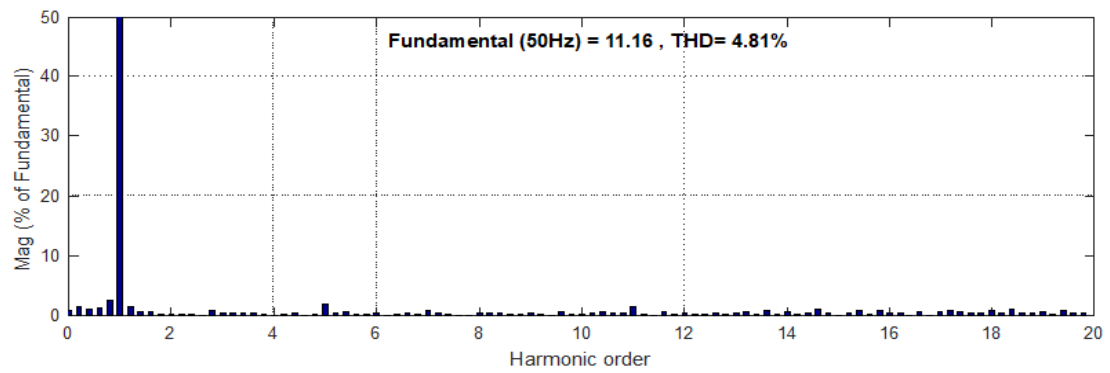
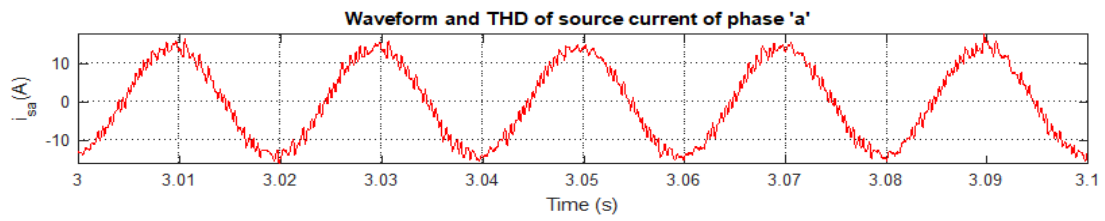
Sr. No.	Generated Power ( $P_g$ )	Load Power ( $P_L$ )	Battery Power ( $P_b$ )
1.	3.700 kW	0.950 kW	2.600 kW
2.	3.500 kW	0.975 kW	2.500 kW
3.	3.000 kW	0.600 kW	2.300 kW

### 5.3.6 Power Quality analysis of distributed generation (DG) system under nonlinear load

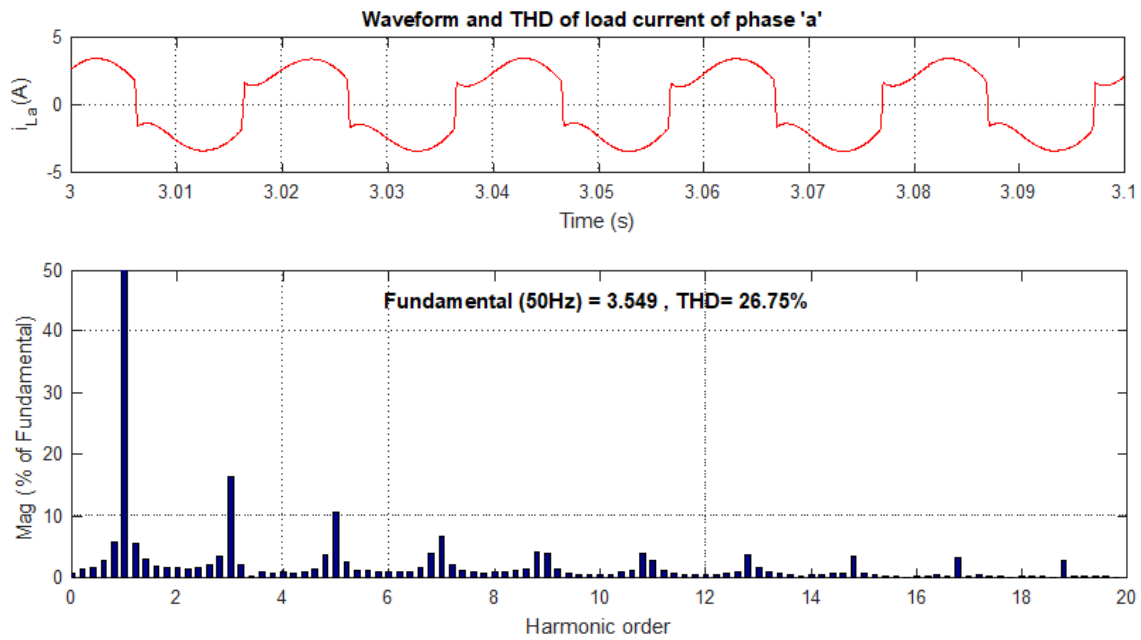
Fig 5.8 (a)-(c) show the waveforms and their respective THD of (a) source voltage (b) source current and (c) load current respectively under nonlinear load condition of DG system. The THD of source voltage, source current and load current are 3.14%, 4.81% and 26.75% respectively. The values of THD in various waveforms are also provided in the Table 5.2. The THD of source voltage and source current is below 5%, which satisfy the IEEE-519 harmonic standard for distributed system.



(a)



(b)



(c)

Fig. 5.8 (a)-(c) Steady state THD analysis of DG system (a) Source voltage (b) Source current and (c) Load current under nonlinear load condition

Table 5.2 Power Quality Indices in Steady State

Sr. No.	THD in $I_s$	THD in $V_s$	THD in $I_L$
1	4.81 %	4.14 %	26.75 %

## 5.4 Conclusions:

The findings of this chapter are summarized as below:

1. The Modified NLMS control algorithm is mathematically modelled and implemented for power quality improvement in wind energy conversion system operating in standalone mode.
2. The complete system setup including Control Algorithm is modelled in MATLAB/Simulink.
3. The simulation study of the distributed generation system with modified NLMS control is carried out under varying load conditions and simulation results

validates the effectiveness of the control scheme for regulating voltage and frequency and also other power quality parameters. The proposed control algorithm has fast dynamic response and it responds within one cycle to track the load variation under transient conditions.

# CHAPTER 6

## CONCLUSIONS AND FUTURE SCOPE OF WORK

---

### 6.1 Main Conclusions

A three-phase SEIG based distributed generating system with advance control algorithms for improving power quality issues have been designed and studied through simulations in MATLAB/Simulink and also experimental analysis. The main objective of this research work was to discuss the effectiveness of advance control algorithms for control of VSC in SEIG based wind energy system to mitigate power quality issues. The leaky momentum control algorithm is described and implemented in wind based distributed energy system which is vulnerable to random variations in wind speed and loads. The LMA has shown capability for regulation of voltage and frequency of the system. It also mitigates the problems of harmonic injections, reactive power compensation and load unbalancing. The LMA is capable in effective elimination of harmonics in the source current which are found to be less than 5% and it is within acceptable range as per IEEE standards-519. This algorithm is able to adopt a suddenly changing wind conditions and load variations. In dynamic conditions it is observed that the dc link voltage of VSC has been maintained within the specified limits. The proposed control scheme is having notable higher convergence rate and faster dynamic response. The 3-phase DG system consisting of a wind driven SEIG with BES has capability to store excess power generation and also deliver power to load during lower wind speed. A modified NLMS control algorithm with VSC is also implemented to work as a harmonic eliminator, regulate the magnitude of source voltage at PCI, active/reactive power support, load leveling, neutral current compensation and other power quality issues in the standalone system. The fundamental weight components for requisite active and reactive component of current are evaluated using a fast, accurate modified-NLMS control algorithm using sensed load current



of the DG system. The BES is interfaced at the DC link of the VSC, which consumes the extra power during less load demand and maintain the power balance between the source and load. The DG system performance is studied under steady-state condition as well as under the perturbation in wind and variation in the nonlinear loads and the performance of SEIG is found satisfactory in standalone operating conditions. The THD of source voltage/current is below 5%, which satisfy the IEEE standard-519.

## **6.2 Future Scope of the work**

The scope of the future works may include the implementation and modelling of some new topology based on types of generators as well as voltage source converter. In addition, some new control algorithms such as adaptive controllers, passivity principle-based controllers, PLL less based controllers, model predictive based controller etc. may be explored to operate the voltage source converter in distributed generation system for regulation of voltage, frequency and improving power quality issues. Further, the research work can be also carried out with microgrid configuration where two to three optimized controllers can be used for parallel interface.

## APPENDIX A

---

### **A1. Rating and Parameters of three Phase SEIG**

Ratings: 3.7 kW, 230 V, 50 Hz and 4-pole; 1440 rpm, Parameters: stator resistance per phase  $R_s = 2.93 \Omega$ , Mutual inductance  $=0.0267544$  H, Rotor resistance  $R_r = 0.4816 \Omega$ , Rotor inductance  $L_r = 0.002016$  H, Inertia constant (H)  $=0.0011$  J (Kg m<sup>2</sup>), Friction  $=0.0023$ ; Excitation capacitor ( $C_{eg}$ ) = 4000 VAR;

**A2. Compensator/VSC parameters:**  $L_s = 10$ mH;  $C_{dc} = 2300$  $\mu$ F, Six IGBT having 1200V, 50A.

**A3. BESS Parameters:** Lithium-ion type, 400V, 7.5AH, SOC (10% to 90%),  $r_s = 0.05\Omega$

**A4. Non-linear load in Phase 'a', 'b' and phase 'c':** Three Single phase Diode bridge Rectifier with dc side load components  $R = 30 \Omega$ ,  $L = 100$  mH.

**A5. Wind Turbine simulation Parameters [3]:**  $P_w = 5$ kW, Radius of turbine blades  $r = 1.4$ m,  $c_p(\lambda, \beta) = 0.87$ ,  $V_w = 12.5$  m/s and  $\rho = 0.48$ .

## List of Publications

1. **Duli Chand Meena**, Madhusudan Singh and Ashutosh K. Giri, “Leaky-momentum control algorithm for voltage and frequency control of three-phase SEIG feeding isolated load” *Journal of Engg. Research ICARI Special Issue*, pp. 109-120 DOI: 10.36909/jer.ICARI.15335. (SCIE Indexed)
2. **Duli Chand Meena**, Madhusudan Singh and Ashutosh K. Giri, “A Modified NLMS Control Algorithm for Coordinated Operation in Three-Phase Wind-Energy Conversion System”, *International Journal of Renewable Energy Research*, Vol. 11, No. 4, pp. 1621- 1629, December,2021 (ESCI/Scopus Indexed)
3. **Duli Chand Meena**, Madhusudan Singh, “Capacitance and Speed Estimation for Self-Excited Induction Generator under Various Loading Conditions”, *3<sup>rd</sup> IEEE Inter. Conf. on Advances in Computing, Communication Control and Networking (ICAC3N-21)*, December, 17<sup>th</sup> -18<sup>th</sup>, 2021. (Presented).

## Authors Biography

### **Duli Chand Meena**

Phone: 9868584955,

Email: [dcmeena@dce.ac.in](mailto:dcmeena@dce.ac.in), [dcmeena\\_dce@yahoo.coms](mailto:dcmeena_dce@yahoo.com)

### **Qualifications:**

B.Tech (NIT-Kurukshetra), M.Tech.(NIT-Kurukshetra), Ph.D ( DTU)

### **Areas of Interest:**

Power Systems, Self-Excited Induction Generator (SEIG), Control of Electrical Machines and Power quality.

**Membership of Professional Societies:** Member IEEE (Membership No. 92972384).

## REFERENCES

- [1] A.R. Jha, *The Wind Turbine Technology*, London, U.K.: CRC Press, 2011.
- [2] M. Godoy Simoes and F.A. Farret, *Alternate Energy Systems, Design and Analysis with Induction Generators*, 2nd ed. London, U.K.: CRC Press, 2008.
- [3] M. Stiebler, *Wind Energy Systems for Electric Power Generation, Green Energy-I and Technology*, Berlin, Germany: Springer- Verlag, 2008.
- [4] A. M. Borbely and Jan F. Keider, *Distributed Generation: The Power Paradigm for the New Millenium*, Boca Raton, FL, USA, CRC Press, 2001.
- [5] L. L. Lai and T. F. Chan, “Distributed Generation: Induction and Permanent Magnet Generator Magnet Generators”. 1st ed. Hoboken, NJ, USA: Wiley, 2007.
- [6] H. Akagi, E. H. Watanable and M. Aredes, “Instantaneous Power Theory and Applications to Power Conditioning” Hoboken, NJ, USA: Wiley, 2007.
- [7] N. Hatziargyriou, ‘Microgrids Architectures and Control’, 1st ed. Hoboken, NJ, USA: Wiley, 2014.
- [8] Bhim Singh, A. Chandra and K. Al-Haddad, “Power quality: Problems and Mitigation Techniques”, Hoboken, NJ, USA: Wiley, 2014.
- [9] B. Singh, S. S. Murthy and S. Gupta, “Analysis and Design of Electronic Load Controller for Self-Excited Induction Generators”, *IEEE Transactions on Energy Conversions*, vol. 21, no. 1, pp. 285–293, 2006.

- [10] R. R. Chilipi, B. Singh, S. S. Murthy and S. Madishetti, “Design and implementation of dynamic electronic load controller for three-phase self-excited induction generator in remote small-hydro power generation”, IET vol. 8, no. March 2013, pp. 269–280, 2014.
- [11] B. Singh, S. S. Murthy and S. Gupta, “STATCOM-Based Voltage Regulator for Self- Excited Induction Generator Feeding Nonlinear Loads”, vol. 53, no. 5, pp. 1437–1452, 2006.
- [12] V. C. Shekhar, K. Kant, and B. Singh, “DSTATCOM supported induction generator for improving power quality”, IET Renewable Power Generation, vol. 10, no. 4, pp. 495–503, 2016.
- [13] G. K. Kasal and B. Singh, “Decoupled voltage and frequency controller for isolated asynchronous generators feeding three-phase four-wire loads”, IEEE Transactions on Power Delivery, vol. 23, no. 2, pp. 966–973, 2008.
- [14] Sabha Raj Arya, Bhim Singh, Ram Niwas, Ambrish Chandra and Kamal Al-Haddad, “Power –Quality Enhancement using DTATCOM in Distributed Power Generation System”, IEEE International Conference on Power Electronics, Drives and Energy Systems (PEDES) 2014.
- [15] A. K. Giri, S. R. Arya, R. Maurya and B. C. Babu, “Power Quality Improvement in Stand- alone SEIG-Based Distributed Generation System Using Lorentzian Norm Adaptive Filter”, IEEE Transactions on Industry Applications, vol. 54, no. 2, pp. 5256–5266, 2018.

- [16] R.K. Agarwal, I. Hussain and B. Singh, “Implementation of LLMF control algorithm for Three-phase grid-tied SPV-DSTATCOM system”, IEEE Transactions on Industrial Electronics, vol.64, no.9, pp.7414-7424, Sep.2017.
- [17] R. Sharma, W. A. Sethares and J. A. Bucklew, “Analysis of Momentum Adaptive Filtering Algorithms,” IEEE Trans. Signal Process., vol. 46, no. 5, pp. 1430–1434, 1998.
- [18] A. K. Giri, S. R. Arya, R. Maurya, and R. Mehar, “Variable learning adaptive gradient based control algorithm for voltage source converter in distributed generation”, IET Renewable Power Generation, vol. 12, no. 16, pp. 1883–1892, 2018.
- [19] Nishant Kumar, Bhim Singh, Bijaya Ketan Panigrahi and Lie Xu, “Leaky-Least- logarithmic Absolute –Difference-based control algorithm and learning-based InC MPPT Technique for Grid-Integrated PV System”, IEEE Transactions on Industrial Electronics, vol.66,no.11, pp.9003-9012,2019.
- [20] A. K. Giri, S. R. Arya and R. Maurya, “Compensation of Power Quality Problems in Wind-Based Renewable Energy System for Small Consumer as Isolated Loads”, IEEE Transactions on Industrial Electronics, vol. 66, no. 11, pp. 9023–9031, 2019.
- [21] Pedro José dos Santos Neto, Adeon Cecílio Pinto, dos Santos Barros Tércio André and Ernesto Ruppert Filho, “A Proposal to Control Active and Reactive Power in Distributed Generation Systems Using Small Wind Turbines”, IEEE Latin America Transactions, vol. 18, no.10, pp. 1699-1706, 2020.

- [22] Sajjad Makhdoomi Kaviri, Hadis Hajebrahimi, Behzad Poorali, Majid Pahlevani, Praveen K. Jain and Alireza Bakhshai, "A Supervisory Control System for Nanogrids Operating in the Stand-Alone Mode", IEEE Transactions on Power Electronics, vol. 36, no. 3, pp. 2914 – 2931, 2021.
- [23] K. Arthishri, N. Kumaresan, and N. Ammasai Gounden, "Analysis and Application of Three-Phase SEIG with Power Converters for Supplying Single-Phase Grid from Wind Energy", IEEE Systems Journal, vol. 13, no.2, pp.1813 - 1822, 2019.
- [24] P. J. Chauhan and J. K. Chatterjee, "A Novel Speed Adaptive Stator Current Compensator for Voltage and Frequency Control of Standalone SEIG Feeding Three-Phase Four-Wire System", IEEE Transactions on Sustainable Energy, vol. 10, no.1, pp.248 - 256, 2019.
- [25] R. Karthigaivel, N. Kumaresan and M. Subbiah, "Analysis and control of self-excited induction generator converter systems for battery charging applicatios", IET electric power applications, vol. 5, no. 2, pp. 247-257 november 2010.
- [26] Woei-Luen Chen, Yung-Hsiang Lin, Hrong-Sheng Gau and Chia-Hung Yu, "STATCOM controls for a self-excited induction generator feeding random loads", IEEE transactions on power delivery, vol. 23, no. 4, october 2008.
- [27] Bhim Singh, S. S. Murthy and R. S. Reddy chilipi, "STATCOM based controller for a three phase SEIG feeding single phase loads", IEEE transactions on energy conversion, vol. 29, no. 2, june 2014.



- [28] K. Arthisn, K. Anusha, N. Kumaresan and S.S. Kumar, "Simplified methods for the analysis of self-excited induction generator" IET electric power applications, oct. 2017.
- [29] Ashutosh K. Giri, Sabha Raj Arya, Rakesh Maurya and B. Chittibabu, "Control of VSC for enhancement of power quality in off-grid distributed power generation", IET renewable power generation, oct. 2019.
- [30] Sabha Raj Arya and Bhim Singh, "Implementation of kernel incremental metalearning algorithm in distribution static compensator", IEEE transactions on power electronics, vol. 30, no. 3, march 2015.
- [31] S. R. Arya, B. Singh, R. Niwas, A. Chandra and K. Al-Haddad, "Power Quality Enhancement Using DSTATCOM in Distributed Power Generation System," IEEE Transactions on Industry Applications, vol. 52, no. 6, pp. 5203-5212, Dec. 2016.
- [32] B. Singh and S. R. Arya, "Software PLL based control algorithm for power quality improvement in distribution system," 2012 IEEE 5th India International Conference on Power Electronics (IICPE), pp. 1-6, 2012.
- [33] Ashutosh K. Giri, Sabha Raj Arya, Rakesh Maurya and B. Chitti Babu, "VCO-less PLL control-based voltage source converter for power quality improvement in distributed generation system" IET electric power applications, vol. 13, iss. 8, pp. 1114-1124, 2019.
- [34] J.A. Barrado, R. Grino and H. valderrama-Blavi, "Power quality improvement of a standalone induction generator using a STATCOM with battery energy

- storage system”, IEEE transactions on power delivery, vol. 25, no. 4, October 2010.
- [35] R. Ahshan, S. A. Saleh and Abdullah Al-Badi, “Performance Analysis of a dq Power Flow Based Energy Storage Control System for Microgrid Applications”, IEEE Access, vol. 8, pp. 178706-178721, 2020.
- [36] R. Essaki Raj, C. Kamalalannan and R. Karthigaivel, “Genetic algorithm-based analysis of wind-driven parallel operated self-excited induction generators supplying isolated loads”, IET renewable power generation, january 2018.
- [37] Felix Dubuission, M. Rezkallah, A. Chandra, M. Saad and H. Ibrahim, “Control of hybrid wind-diesel standalone microgrid for water treatment system application”, IEEE Transactions on Industry Applications, vol. 55, no. 6, Nov.-Dec. 2019.
- [38] Farheen Chisti and Bhim Singh, “Development of wind and solar based AC microgrid with power quality improvement for local nonlinear load using MLMS”, IEEE transactions on industry applications, vol. 55, no. 6, December 2019.
- [39] V. Narayan, Seema Kewat and Bhim Singh, “MVSS-LMS control for a three-phase standalone solar PV-BES-DG based microgrid”, International transactions on electrical. Energy system, March 2020.
- [40] LI Zhoufan, LI Dan, XU Xinlong and ZHANG Jianqiu, “New normalized LMS adaptive filter with a variable regularization factor”, Journal of systems engineering and electronics, vol. 30, no. 2, pp. 259-269, April 2019.

- [41] S. A. Saleh and R. Ahshan, "Parameter Adjustment for the Droop Control Operating a Discharge PEC in PMG-Based WECSs with Generator-Charged Battery Units", *IEEE Access*, vol. 9, pp. 89064 - 89078, 2021.
- [42] R. Ahshan, M. T. Iqbal, George K.I. Mann, "Controller for a Small Induction Generator Based Wind Turbine", *Applied Energy*, vol. 85(4), pp. 218-227, 2008.
- [43] S. Sombir and Madhusudan Singh, "Voltage and frequency control of self - excited induction generator integrated with PV system", *IECON*, the 46th annual conference of the IEEE industrial electronics society, 978-1-7281-5414-5/20, 2020.
- [44] M. Moradian and J. Soltani, "An Isolated Three phase Induction Generator System With Dual Stator Winding Sets Under Unbalanced Load Condition" *IEEE Transactions on Energy Conversion*, vol. 31, no. 2, pp.531 – 539, 2016.
- [45] E.S. Abdin and W. Xu, "Control design and dynamic performance analysis of a wind turbine-induction generator unit", *IEEE Transactions on Energy Conversion*, vol. 15, no. 1, pp. 91 – 96, 2000.
- [46] Bhim Singh; Madhusudan Singh and A. K. Tandon, "Transient Performance of Series-Compensated Three-Phase Self-Excited Induction Generator Feeding Dynamic Loads", *IEEE Transactions on Industry Applications*, vol. 46, no.4, pp.1271 – 1280, 2010.
- [47] Wagner E. Vanço; Fernando B. Silva; Carlos Matheus R. De Oliveira; José Roberto B. A. Monteiro and José Mário M. De Oliveira, "A Proposal of Expansion and Implementation in Isolated Generation Systems Using Self-

- Excited Induction Generator with Synchronous Generator”, IEEE Access, vol. 7, pp. 117188 – 117195, 2019.
- [48] R.C. Bansal, “Three-phase self-excited induction generators: An overview”, IEEE Transactions on Energy Conversion, vol. 20, no.2, pp. 292 – 299, 2005.
- [49] T. Ahmed; K. Nishida and M. Nakaoka, “Advanced control of PWM converter with variable-speed induction generator” IEEE Transactions on Industry Applications, vol. 42, no.4, pp. 934 – 945, 2006.
- [50] O. Ojo and I.E. Davidson, “PWM-VSI inverter-assisted stand-alone dual stator winding induction generator”, IEEE Transactions on Industry Applications, vol. 36, no. 6, pp. 1604.– 1611, 2000.
- [51] T. Fukami; Y. Kaburaki; S. Kawahara and T. Miyamoto, “Performance analysis of a self-regulated self-excited single-phase induction generator using a three-phase machine”, IEEE Transactions on Energy Conversion, vol. 14, no. 3, pp. 622 – 627, 1999.
- [52] E.G. Marra and J.A. Pomilio, “Self-excited induction generator controlled by a VS-PWM bidirectional converter for rural applications”, IEEE Transactions on Industry Applications, vol. 35, no. 4, pp. 877 – 883, 1999.
- [53] Woei-Luen Chen; Yung-Hsiang Lin; Hrong-Sheng Gau and Chia-Hung Yu, “STATCOM Controls for a Self-Excited Induction Generator Feeding Random Loads”, IEEE Transactions on Power Delivery, vol. 23, no. 4, pp. 2207 – 2215, 2008.
- [54] T. Ahmed; O. Noro; E. Hiraki and M. Nakaoka, “Terminal voltage regulation

- characteristics by static var compensator for a three-phase self-excited induction generator”, *IEEE Transactions on Industry Applications*, vol. 40, no. 4, pp. 978 – 988, 2004.
- [55] J. A. Barrado; R. Grino and H. Valderrama-Blavi, “Power-Quality Improvement of a Stand-Alone Induction Generator Using a STATCOM With Battery Energy Storage System”, *IEEE Transactions on Power Delivery*, vol. 25, no. 4, pp. 2741 – 2741, 2010.
- [56] K. Arthishri;N. Kumaresan and N. Ammasai Gounden, “Analysis and Application of Three-Phase SEIG With Power Converters for Supplying Single-Phase Grid From Wind Energy”, *IEEE Systems Journal*, vol. 13, no. 2, pp. 1813 – 1822, 2019.
- [57] E.G. Marra and J.A. Pomilio, “Induction-generator-based system providing regulated voltage with constant frequency” *IEEE Transactions on Industrial Electronics*, vol. 47, no. 4, pp. 908 – 914, 2000.
- [58] S. Lenin Prakash; M. Arutchelvi and A. Stanley Jesudaiyan, “Autonomous PV-Array Excited Wind-Driven Induction Generator for Off-Grid Application in India”, *IEEE Journal of Emerging and Selected Topics in Power Electronics*, vol. 4, no. 4, pp. 1259 – 1269, 2016.
- [59] M.a. El-Sharkawi; S.S. Venkata; T.J. Williams and N.G. Butler, “An Adaptive Power Factor Controller for Three-Phase Induction Generators”, *IEEE Transactions on Power Apparatus and Systems*, vol. 104, no.7, pp. 1825– 1831, 1985.

- [60] Feifei Bu; Wenxin Huang; Yuwen Hu and Kai Shi, “ An Excitation-Capacitor-Optimized Dual Stator-Winding Induction Generator With the Static Excitation Controller for Wind Power Application”, IEEE Transactions on Energy Conversion, vol. 26, no.1, pp.122 – 131, 2011.
- [61] L.A.C. Lopes and R.G. Almeida, “Wind-driven self-excited induction generator with voltage and frequency regulated by a reduced-rating voltage source inverter”, IEEE Transactions on Energy Conversion, vol. 21, no. 2, pp. 297-304, 2006.
- [62] Ujjwal Kumar Kalla, Bhim Singh and S. Sreenivasa Murthy, “Enhanced Power Generation from Two-Winding Single-Phase SEIG Using LMDDT-Based Decoupled Voltage and Frequency Control”, IEEE Transactions on Industrial Electronics, vol. 62, no. 11, pp. 6934 – 6943, 2015.
- [63] D. Joshi, K.S. Sandhu and M. K. Soni, “Constant voltage constant frequency operation for a self-excited induction generator”, IEEE Transactions on Energy Conversion, vol.21, no.1, pp. 228 – 234, 2006.
- [64] Kodakkal Amritha, Veramalla Rajagopal, Kuthuri Narasimha Raju and Sabha Raj Arya, “Ant lion algorithm for optimized controller gains for power quality enrichment of off-grid wind power harnessing units”, Chinese Journal of Electrical Engineering, vol. 6, no. 3, pp. 85 – 97, 2020.
- [65] Feifei Bu, Wenxin Huang, Yuwen Hu and Kai Shi, “An Integrated AC and DC Hybrid Generation System Using Dual-Stator-Winding Induction Generator With Static Excitation Controller”, IEEE Transactions on Energy Conversion, vol. 27, no. 3, pp. 810 – 812, 2012.

- [66] Juan M. Ramirez and Emmanuel Torres M, “An Electronic Load Controller for the Self-Excited Induction Generator”, *IEEE Transactions on Energy Conversion*, vol. 22, no. 2, pp. 546 – 548, 2007.
- [67] P. J. Chauhan, J. K. Chatterjee, Haresh Bhare, B. V. Perumal and Dipankar Sarkar, “Synchronized Operation of DSP-Based Generalized Impedance Controller With Variable-Speed Isolated SEIG for Novel Voltage and Frequency Control”, *IEEE Transactions on Industry Applications*, vol. 51, no. 2, pp. 1845 – 1854, 2015.
- [68] W.L. Chen and Y.Y. Hsu, “Unified voltage and pitch angle controller for wind-driven induction generator system”, *IEEE Transactions on Aerospace and Electronic Systems*, vol. 44, no. 3, pp. 913 – 926, 2008.
- [69] Athira G. S, Archana C. M, R. Sudharshan Kaarthik and Rajeevan P. P, “An Induction Generator Scheme With Series-Compensation for Frequency Insensitive Loads”, *IEEE Transactions on Industrial Electronics*, vol. 68, no. 9, pp. 8402 – 8411, 2021.
- [70] Ioannis D. Margaritis, Stavros A. Papathanassiou, Nikos D. Hatziargyriou, Anca D. Hansen and Poul Sorensen, “Frequency Control in Autonomous Power Systems With High Wind Power Penetration”, *IEEE Transactions on Sustainable Energy*, vol. 3, no. 2, pp. 189 – 199, 2012.
- [71] D. Mascarella, P. Venne, D. Guérette and G. Joos, “Flicker Mitigation via Dynamic Volt/VAR Control of Power-Electronic Interfaced WTGs”, *IEEE Transactions on Power Delivery*, vol. 30, no. 6, pp. 2451 – 2459, 2015.

- [72] Bjarti Thomsen, Josep M. Guerrero and Paul B. Thøgersen, “Faroe Islands Wind-Powered Space Heating Microgrid Using Self-Excited 220-kW Induction Generator”, *IEEE Transactions on Sustainable Energy*, vol. 5, no.4, pp. 1361 – 1366, 2014.
- [73] Ujjwal Kumar Kalla, Bhim Singh and S. S. Murthy, “Intelligent Neural Network-Based Controller for Single-Phase Wind Energy Conversion System Using Two Winding Self-Excited Induction Generator”, *IEEE Transactions on Industrial Informatics*, vol. 12, no. 6, pp. 1986 – 1997, 2016.
- [74] Faa-Jeng Lin, Po-Kai Huang, Chin-Chien Wang and Li-Tao Teng, “An Induction Generator System Using Fuzzy Modeling and Recurrent Fuzzy Neural Network”, *IEEE Transactions on Power Electronics*, vol. 22, no. 1, pp. 260 – 271, 2007.
- [75] Dominik A. Górski and Grzegorz Iwański, “Asynchronous Grid Connection of a Cage Induction Generator Excited by a Power Electronic Converter”, *IEEE Transactions on Energy Conversion*, vol. 36, no. 1, pp. 63 – 70, 2021.
- [76] G. Raina, O.P. Malik, “Wind Energy Conversion Using a Self Excited Induction Generator,” *IEEE Transactions on Power Apparatus and Systems*, Vol. PAS 102, No.12, pp. 3933-3936, December 1983.
- [77] A. S. Abdel-Karim, S.A. Hassan and S. S. Shakralla, “Power generation by wind energy systems using induction generators”, *Proc. 2nd National Power System Conf.*, Hyderabad, India, pp. 43–50, Sep., 1993.
- [78] R. C. Bansal, T. S. Bhatti, and D. P. Kothari, “A bibliographical survey on induction generators for application of nonconventional energy systems”,



- IEEE Trans. Energy Convers., vol. 18, no. 3, pp. 433–439, Sept. 2003.
- [79] J. M Chapallaz, J. Ghali, P. Eichenberger and G. Fischer, “Manual on Induction Motors Used as Generators”, Vol.10, 1992.
- [80] T. F. Chan and L. L. Loi, “Capacitance requirements of a three-phase induction generator self-excited with a single capacitance and supplying a single-phase load,” IEEE Trans. Energy Conversion, vol. 17, pp. 90–94, Mar. 2002.
- [81] B. Venkatesa Perumal and Jayanta K. Chatterjee, “Voltage and Frequency Control of a Stand-Alone Brushless Wind Electric Generation Using Generalized Impedance Controller”, IEEE Transactions on Energy Conversion, vol. 23, no. 2, June 2008.
- [82] Rajasekhara Reddy Chilipi, Bhim Singh, and S. S. Murthy “Performance of a Self-Excited Induction Generator With DSTATCOM-DTC Drive-Based Voltage and Frequency Controller”, IEEE Transactions on Energy Conversion, vol. 29, no. 3, September 2014.
- [83] D. C. Meena, M S Singh and A. K. Giri, “Leaky-momentum control algorithm for voltage and frequency control of three-phase SEIG feeding isolated load”, Journal of Engg. Research ICARI Special issue, pp 109-120, Oct. 2021.
- [84] S. S. Murthy, B. P. Singh, C. Nagamani and K.V.V. Satyanarayna, “Studies on the use of conventional induction motors as self-excited induction generator”, IEEE Trans. Energy Conversion, vol. 3, pp. 842 – 848, 1988.
- [85] Sharad Rajan.: Steady State Performance Evaluation of Self Excited Induction Generator for SHP. Dissertation IIT-Roorkee, 2012.

- [86] D. K. Jain, A. P. Mittal and Bhim Singh, "A New Iterative Technique for The Steady State Analysis of Three Phase Self-Excited Induction Generator", 10th National Power Systems Conference, MS Univerity of Baroda, Vadadora, India, 1998.
- [87] Krishnan Arthishri, Kumaresan Anusha, Natarajan Kumaresan and Subramaniam Senthil Kumar, "Simplified methods for the analysis of self-excited induction generators", IET Electric Power Applications, July 2017.
- [88] Swarup Kumar Saha and Kanwarjit Singh Sandhu, "Optimization Techniques for the Analysis of Self-excited Induction Generator," 6th International Conference on Smart Computing and Communications, (ICSCC), December 2017.
- [89] Yatender Chaturvedi, Sumit Kumar, Priti Bansal and Sushil Yadav, "Comparison among APSO, PSO & GA for Performance Investigation of SEIG with Balanced Loading," IEEE 9th international conference on cloud computing, Data Science and Engineering (Confluence)), Jan.2019
- [90] J. J. Shynk and S. Roy, "The LMS Algorithm with Momentum updating", IEEE Symposium on Circuits and Systems, pp.2651- 2654, 1988
- [91] S. Roy and J. J. Shynk, "Analysis of the momentum LMS algorithm," IEE Trans. Acoust., Speech, Sig. Proc., submitted 1988.
- [92] L. L. Horowitz and K. D. Senne, "Performance advantage of complex LMS for controlling narrow-band adaptive arrays," IEEE Trans. Circuits Systems, vol. CAS-28, no. 6, pp. 562-576, June 1981.

- [93] S. S. Haykin, Adaptive Filter Theory. Englewood Cliffs, 4<sup>th</sup> ed. Upper Saddle Rier, New Jersey: Prentice -Hall, 2002.
- [94] B. Widrow and S. D. Stearns, Adaptive Signal Processing. Englewood Cliffs, New Jersey: Prentice-Hall, 1985